RSC Advances

ROYAL SOCIETY OF CHEMISTRY

www.rsc.org/advances

Journal Name

RSCPublishing

In vitro and *in vivo* cytocompatibility of electrospun nanofiber scaffolds for tissue engineering applications

Cite this: DOI: 10.1039/x0xx00000x

N. Goonoo[a], A. Bhaw-Luximon[a] and D. Jhurry[a*]

Received 00th January 2012,
Accepted 00th January 2012

DOI: 10.1039/x0xx00000x

www.rsc.org/

The use of polymeric-based nanofibers has gained more and more attention during the past decade in the biomedical and pharmaceutical fields and as a result, nanotoxicology research is inevitable to satisfy the requirements of regulating agencies such as FDA as well as biosafety needs. Recent advances have witnessed the emergence of an increasing number of nanosized materials. While the number of potential applications related to the use of electrospun nanofibers continues to increase, studies to characterize their effects after exposure and to address their potential cytocompatibility are few in comparison. A comprehensive understanding of nano-bio and physico-chemical interactions is necessary from the early stage of nanomaterial conception to prevent pitfalls of materials failure at preclinical and clinical stages. This review presents a summary of both *in vitro* and *in vivo* cytocompatibility data currently available on synthetic and natural polymer-based electrospun nanofibers under investigation for tissue engineering applications. Cellular response dependence on cell type and nature of scaffold is also addressed.

Introduction

Over the past few years, electrospinning has grown from a small niche process to a widely used fiber fabrication technique. Major applications of electrospun fibers include tissue engineering, controlled drug delivery, sensing, separations, filtration, catalysis and nanowires [1].

Several excellent reviews have been published on electrospinning and the use of electrospun nanofibers [2-6]. Huang *et al.* [5] stressed on developments related to electrospun polymer nanofibers including processing, structure and property characterization, applications as well as modelling and simulations. Xie *et al.* [7] focused on the attributes of electrospun nanofibers which make them suitable for a range of biomedical applications including drug delivery and tissue engineering. Indeed, the high porosity, large surface area and the possibility of functionalization of nanofibers through encapsulation or attachment of bioactive species allow them to serve as ideal scaffolds, mimicking the extracellular matrix (ECM) of the target tissue. Furthermore, nanofibers have been highlighted as promising candidates for bone, cartilage, vascular, neural and bladder tissue engineering applications [8]. The potential risk and toxicity of nanomaterial synthesis as well as its use related to human health were also identified as an important future area of research [8].

Recently, much attention has been given to cytocompatibility testing of electrospun nanofibers. Nanofiber matrices support cell attachment and proliferation, and at the same time maintain cell phenotypes. In a comprehensive review by Nisbet *et al.* [9], cellular interactions with electrospun scaffolds, with particular focus on neural, bone, cartilage, and vascular tissue regeneration were addressed. Aspects of scaffold design, including architectural properties, surface functionalization and materials selection were also highlighted. The use of nanostructures in the creation of the next generation of biomaterials with well-defined nanotopography capable of eliciting the desired cellular and tissue response has been reviewed by Kim *et al.* [10]. Cytocompatibility experiments conducted on nanofibers were briefly discussed by Ma *et al.* [11]. In an exhaustive review on the design, fabrication and use of PCL scaffolds for tissue engineering applications, Cipitria *et al.* summarized the knowledge about factors affecting cellular responses such as mesh morphology, topography, chemistry and mechanical properties [12].

A number of clinical applications for electrospun fibers are currently being considered. Preliminary studies have demonstrated that a range of electrospun nanofibers showed no toxicity towards living cells, no inflammatory response or loss of cell integrity, as well no cellular damage. Cells and scaffolds are the two major elements for successful tissue engineering [13]. Due to the unique capabilities of stem cells such as self-renewal and multi-lineage differentiation, the combination of stem cells and nanofibrous scaffolds have become the focal point of many investigations [13,14]. The latest review paper on biocompatibility and cellular response of nanofibers dates back to 2011 whereby *in vitro* and *in vivo* studies on electrospun nanofibrous scaffolds have been presented, however limited to PCL and PCL blend mats [12]. The authors stressed on the physical and chemical characterization of electrospun mats and on thorough reporting of experimental parameters regarding cytocompatibility studies for a better comparison among laboratories.

As nanofibers for tissue engineering applications move towards the use of blends of natural and synthetic polymers, a review of the status of cytocompatibility and cytotoxicity studies on a range of polymers belonging to these categories

would serve the community of researchers and engineers. After a preliminary presentation of *in vitro* cytotoxicity assays including microscopy and spectrophotometric measurements, *in vivo* evaluation of biomaterials correlated with factors affecting cellular responses of electrospun nanofibers such as surface roughness, fiber alignment, fiber composition are here highlighted. Cellular response based on cell type and nature of scaffold is also here reviewed.

General Background: Biocompatibility and Cellular Response

Tissue engineered polymeric-based scaffolds are an integral part of future regenerative efforts and as reported in our recent review, biocompatibility, biodegradability and mechanical performance of the polymers highly impact on the scaffolds [15]. Cells sense and respond to the physical properties of the matrix by converting mechanical cues into intracellular chemical signals, which in turn, control gene expression, protein production and phenotypic behavior. According to the International Standard ISO 10993 (Biological Evaluation of Medical Devices), all materials used in humans are subjected to *in vitro* and *in vivo* biocompatibility tests to verify response and behavior of cells interacting with them. A material is said to be biocompatible when the latter interacts with the body without inducing unacceptable toxic, immunogenic, thrombogenic and carcinogenic responses, and any other side effects. The complex and dynamic cell-ECM communication takes place through both integrin and non-integrin membrane bound receptors (Figure 1). Fibronectin and integrins play crucial roles in a variety of morphogenetic processes, in which they mediate cell adhesion, migration and signal transduction [17]. Integrins cluster in specific cell-matrix adhesions to provide dynamic links between extracellular and intracellular environments by bi-directional signalling and by organizing the ECM and intracellular cytoskeletal and signalling molecules [18,19]. Initially, cell adhesion to the ECM is induced by multiple, low affinity charge and hydrophobic interactions. The spreading phase of cell adhesion is induced by integrins on the cell surface which bind to specific small peptide fragment sequences on the ECM. This allows cell attachment to the ECM through focal adhesions and promotes direct communication between the two.

The different ECM components like laminin, fibronectin, and collagen type I interact differently with cell behavior patterns: attachment dynamics such as adhesion kinetics and force, formation of focal adhesion complexes, morphology, proliferation, and intercellular communication. Schlie-Wolter *et al.* carried a detailed *in vitro* comparison of fibroblasts, endothelial cells, osteoblasts, smooth muscle cells, and chondrocytes which showed significant differences in their cell responses to the ECM: cell behavior follows a cell specific ligand priority ranking, which was independent of the cell type origin. Fibroblasts responded best to fibronectin, chondrocytes best to collagen I, the other cell types best to laminin [20]. This knowledge is essential for optimization of tissue-biomaterial interfaces in all tissue engineering applications and gives insight into tissue-specific cell guidance [20].

Biocompatibility is a term that encompasses cytocompatibility and cytotoxicity [21]. Cytocompatibility involves testing of the material in contact with cells. Cytotoxicity, on the other hand, deals mainly with the substances that leach out of the materials for instance degradation products. Cytotoxicity testing relies more on biochemical tests, while cytocompatibility is evaluated through cell morphological changes.

Evaluating the biocompatibility of materials has been a complex task. This complexity arises from the fact that materials have various intended uses, with body contact ranging from transient skin contact to contact with blood to permanent implantation. Biocompatibility is generally demonstrated by testing materials, and their leachable chemicals, using toxicological principles. The biomaterials should not—either directly or through the release of their constituents—produce adverse local or systemic effects, be carcinogenic, or produce adverse reproductive and developmental effects. Therefore, evaluation of any material intended for human use requires data from systematic testing to ensure that the benefits provided by the final product will exceed any potential risks posed by device materials.

A number of factors need to be addressed when evaluating the biocompatibility of a material. Firstly, biocompatibility is highly anatomically dependent which means that the reactions to a particular material vary from one location to another [22-23]. Often, drug/gene eluting vascular grafts are fabricated to enhance vascular cell attachment. In such cases, it is crucial to consider the drug release aspect. For instance, a material may not cause any tissue injury at all but nonetheless kill the animal, either from drug release [24] or from some unforeseen side effects such as intravascular coagulation [25], embolic events [26], chelation of ions vital to homeostasis, etc. It is therefore important to consider that the drug itself can have important effects on the biocompatibility especially for formulations involving a stationary depot. Porosity and surface modification of polymers are important features that need to be taken into consideration in promoting biocompatibility of a scaffold [27]. Since scaffolds are specifically designed to interact with cells, it is important to ensure that these enhancements do not cause any adverse effects. It is also crucial to consider biodegradation of scaffolds and the cellular responses induced by the degraded products. For instance, in the case of nanoparticles, it has been reported that biodegradation leads to intracellular changes such as disruption of organelle integrity or gene alterations [28].

Generally, the biocompatibility of a material is evaluated through both *in vitro* and *in vivo* phases. *In vitro* studies provide a rough assessment of the ability of relevant cell types to survive in the presence of a material. This can be achieved using a number of tests such as the MTT assay, measures of DNA synthesis and cell proliferation, and dye-based cell membrane integrity tests [29]. It may be useful to assess the effects of both direct contact with cells and indirect exposure to diffusible components (residual solvents or monomers, breakdown products, drugs, acid etc.). Even though, cell-based models used *in vitro* accurately reflect their counterparts inside the body, they do not take the rest of the body into account. Hence, *in vivo* studies are equally important. A material may not be directly cytotoxic to particular cells, but may yet induce a reaction that is destructive at other locations. An accurate and precise *in vitro* cytotoxicity assay can decrease the number of animal studies required to develop a new medical device or implanted biomaterial [30]. At the same time, they should be sufficiently rapid to allow screening of large numbers of potential biomaterials.

Cytotoxicity or biocompatibility is usually decided by the natural property of the material. Polyesters (polycaprolactone (PCL), poly(lactides) (PLAs)), poly(ester-ethers) (polydioxanone (PDX)) and their copolymers are the most widely used biocompatible scaffolds. Poly(lactide-*co*-glycolide) (PLGA) is one of the most commonly known FDA-approved materials with excellent biocompatibility. However, when fabricated into electrospun mats, they degrade faster due to higher surface area to volume ratio [31] and the degradation products affect cellular responses. Indeed, better scaffold mineralization was observed for PDX containing 50% HA compared to the corresponding PLGA scaffolds in ionic simulated body fluid (i-SBF) and revised simulated body fluid (r-SBF) as shown by Madurantakam *et al.* [32]. This clearly shows that the acidic degradation products of PLGA inhibited mineral growth on the scaffolds. The creation of an ECM analogue is extremely challenging, yet possible, may be through the use of natural polymers since they possess the signalling capabilities normally required by cells [33]. The primary goal is to minimize the risk of rejection or failure by regulating the response such that it promotes healing [34-35].

Journal Name RSCPublishing

Cell – ECM communication
Adhesion, Proliferation, Migration, Survival

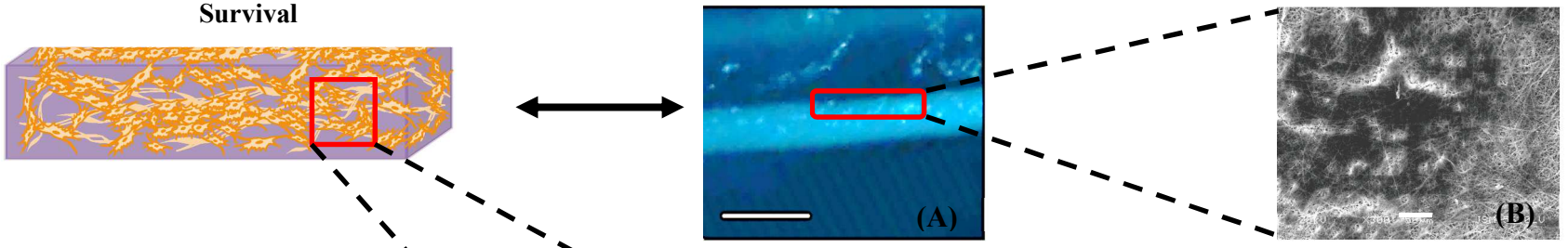

Cell growth on electrospun nanofibrous scaffold mimicking the ECM (A) Fluorescence image showing cross-sectional view (scale bar 200 µm) and (B) SEM image (600X magnification, scale bar 20 µm)

Integrins - heterodimeric transmembrane receptors providing a physical and biochemical bridge between components of the ECM and the intracellular physiological environment. Binding of integrins to their ligands results in the formation of cytoplasmic multi-protein assemblies composed of both cytoskeletal and signalling molecules.

Cell membrane - semi-permeable membrane surrounding the cytoplasm of a cell.

Collagens - most abundant components of ECM and many types of soft tissues.

Fibronectin - "master organizer" in matrix assembly as it forms a bridge between cell surface receptors, e.g. integrins and compounds such collagen and other focal adhesion molecules.

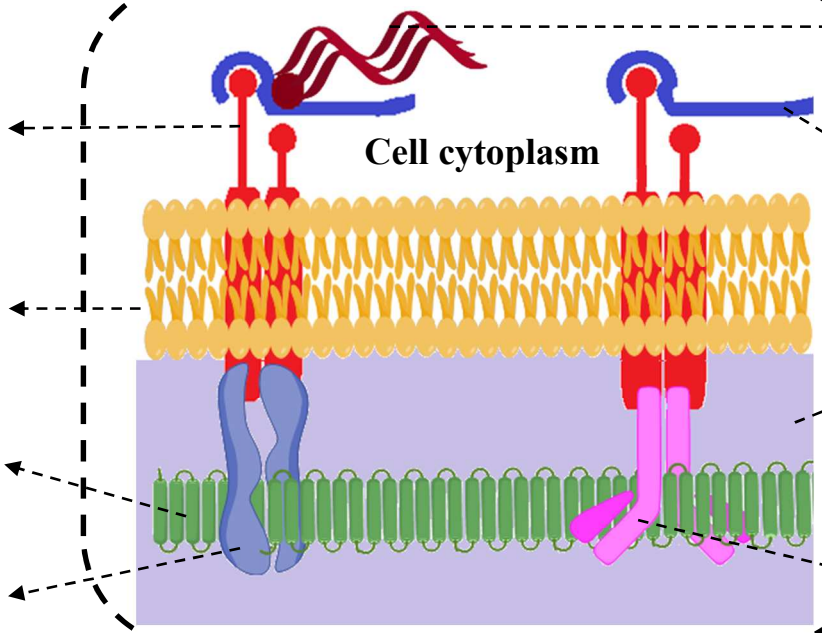

Actin filaments - thin, flexible fibers providing mechanical support, determining cell shape, and allowing movement of the cell surface.

Adaptor proteins - control the activity of a series of signal transduction pathways.

ECM- non-cellular component present within all tissues and organs that provides structural and biochemical support to surrounding cells.

Laminin - contribute to the structure of ECM and modulate cellular functions such as adhesion, differentiation, migration, stability of phenotype, and resistance towards apoptosis.

Figure 1: Cell-ECM communication (SEM and fluorescence image adapted from Biomater Sci [16])

Journal Name RSCPublishing

Bio-testing of Biomaterials

Biocompatibility tests generally include two levels: (i) biosafety testing and (ii) bio-functional testing [36]. In biosafety tests, the materials are tested for their toxicity to cultured cells, haemolysis or allergic responses, or whether they induce heritable genetic alterations or tissue necrosis after animal implantation. The second level testing focuses on the specific functions of a biomaterial, in which the responses of all the cell and tissue types in contact with the material are investigated using both *in vitro* and *in vivo* methods. Advantages of *in vitro* tests include low costs, quick turnover and high throughput screening. *In vivo* tests, on the other hand, provides multi-system interactions. In addition, it is costly, has low turnover (weeks to months), low throughput, and has animal use concerns [37].

Cytotoxicity Assays For Nano-biomaterials

Williams [38] defined the biocompatibility of a scaffold as follows: "*The biocompatibility of a scaffold or matrix for a tissue engineering product refers to the ability to perform as a substrate that will support the appropriate cellular activity, including the facilitation of molecular and mechanical signalling systems in order to optimize tissue regeneration, without eliciting any undesirable local or systemic responses in the eventual host*". For many years, cell culture methods have been used to understand how a potential biomaterial will react in the body. Several major cell types are used for *in vitro* testing, including phagocytic, neural, hepatic, epithelial, endothelial, red blood cells and various cancer cell lines. The specific cell line selected for *in vitro* assay is intended to model a response likely observed or sensitized by particles *in vivo* [39]. Cell cultures are sensitive to changes in their environment such as changes in temperature, pH and nutrient and waste concentrations as well as the concentration of the potentially toxic agent being tested [28]. Therefore, it is crucial to control the experimental conditions to ensure that the measured cell death corresponds to the toxicity of the added electrospun nanofibers versus the unstable culturing conditions. Three cell culture assays are usually used to evaluate biocompatibility including direct contact, agar diffusion and elution as described in standards published by ASTM, ISO, and BSI [40]. They are all morphological assays which mean that the outcome is measured by the observations of changes in cell morphology. L-929 mouse fibroblast cells are the most extensively used cells in biomaterials evaluation because they are easy to maintain and produce results with high correlation with animal bioassays. Furthermore, fibroblasts are one of the first cells to invade the wound healing area and a major cell in tissue attachment to biomaterials.

Microscopy

One simple cytotoxicity test involves visual inspection of the cells with bright-field microscopy for changes in cellular or nuclear morphology. Usually, the cells are stained with a fluorescent dye such as 4',6-diamidino-2-phenylindole (DAPI) or Hematoxylin and Eosin stain (H&E) [41-43]. DAPI is a fluorescent stain that binds strongly to A-T rich regions in DNA. For example, DAPI and H&E staining of fibroblasts cultured on electrospun 80/20 elastin/collagen scaffold showed cell infiltration of about 150 μm throughout the scaffold [42]. However, the majority of cytotoxicity assays used for electrospun nanofibers measure cell death via colorimetric methods. These colorimetric methods can be further categorized into tests that measure plasma membrane integrity and mitochondrial activity.

The LIVE/DEAD viability test is another assay measuring the number of damaged cells [44-45]. Cells are stained with calcein acetoxymethyl (calcein AM) and ethidium homodimer and viewed under a microscope. Calcein AM is an electrically neutral esterified molecule which can easily penetrate cells through diffusion. It is then converted to calcein, a green fluorescent molecule by intracellular esterases inside cells. Damaged or dead cells, on the other hand, are stained by ethidium homodimer, a membrane impermeable molecule and fluoresce red when the dye binds to nucleic acids. Calcein AM and ethidium homodimer emit distinct fluorescence signatures at 515 nm and 635 nm respectively when excited at 495 nm [46]. Figure 2 shows the micrographs of live/dead staining of osteoblasts on electrospun PHBV/silk/n-HA.

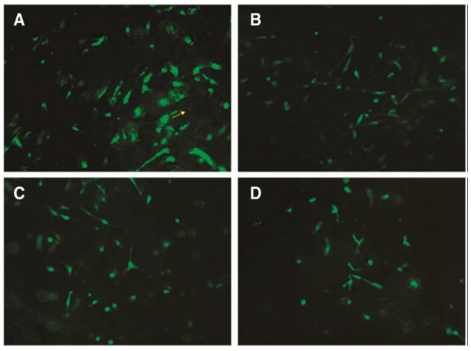

Figure 2: Microscopic micrographs of live/dead staining after 1 day (A, C) and 3 days (B, D): A-control P0 (1 day), B- control P0 (3 days), C- P5 (1 day), D- P5 (3 days). Live cells are stained green and dead/damaged cells are stained red (original magnification 10×). (yellow arrow indicates the dead cells visualized in red colour). Reprinted with permission from [45], E. I. Paşcu, J. Stokes and G. B. McGuinness, *Materials Science and Engineering C* 2013, 33, 4905. © 2013, Elsevier.

Metabolic activity tests

Exposure to certain cytotoxic agents can compromise the cell membrane, which allows cellular contents to leak out [28]. Quantitative viability tests based on this include the neutral red [47], Trypan blue assays. Neutral red or toluylene red, is a weak cationic dye that can cross the plasma membrane by diffusion. This dye tends to accumulate in lysosomes within the cell. If the cell membrane is altered, the uptake of neutral red is decreased and can leak out, allowing for discernment between

live and dead cells. Cytotoxicity can be quantified by taking spectrophotometric measurements of the neutral red uptake at 540 nm. Intensity of the red colour obtained is proportional to the viability of the cell population and inversely proportional to the cytotoxicity of scaffolds.

Resazurin or alamar blue is another commonly used colorimetric assay where the non-fluorescent alamar blue dye is reduced to a pink fluorescent dye by cell metabolic activity mainly by acting as an electron acceptor for enzymes such as NADP and FADH during oxygen consumption [48-49].

Lactate dehydrogenase assay

Another cytotoxicity assay used is lactate dehydrogenase (LDH) release monitoring. In this assay, LDH released from damaged cells oxidizes lactate to pyruvate, which promotes conversion of tetrazolium salt INT to formazan, a water-soluble molecule with absorbance at 490 nm. The amount of LDH released is proportional to the number of cells damaged or lysed [50].

MTT and MTS assays

In addition to distinguishing between live and dead cells, other colorimetric cytotoxicity assays try to determine the mechanism behind the induced cell death [28]. The most widely used tests are the MTT [51-57] and MTS [58-60] viability assays. Metabolically active cells react with tetrazolium salts as mitochondrial dehydrogenase enzymes and cleave the tetrazolium ring. Only active mitochondria contain these enzymes and therefore, the reaction occurs only in living cells. MTT (3-(4,5-dimethylthiazol-2-yl)-2,5-diphenyl tetrazolium bromide) is pale yellow in solution but produces a dark-blue formazan product within live cells. MTS (3-(4,5-dimethylthiazol-2-yl)-2,5-diphenyltetrazolium bromide), on the other hand is reduced from yellow to purple formazan in living cells. The number of living cells can be determined by quantifying the production of formazan by measuring the absorbances at 620 and 492 nm for MTT and MTS assays respectively [61]. Another example of tetrazolium-based assay used to test cytotoxicity is the WST assay. WST-1 or WST-8 is converted to a yellow-orange coloured formazan product, which can be quantified at 450 nm [62].

Other tests

Cell adhesion is an important factor when evaluating the integration of implanted biomaterials. The Actin Cytoskeleton & Focal Adhesion Staining Kit (Millipore, USA) can be used to investigate the cytoskeletal organization and focal adhesion [63].

Inflammation is also a possible adverse effect of exposure to electrospun nanofibers. Commonly tested pro-inflammatory cytokines or protein signals of inflammatory response include IL-1b, IL-6, and TNF-a plus the chemokine IL-8 [64-65]. These cytokines are detected using enzyme-linked immunosorbant assay (ELISA) and can be quantified by measuring the absorbance from either alkaline phosphatase or strepavidinhorseradish peroxidase labelled antibodies at 405 or 620 nm, respectively [66].

Flow cytometric analysis is used to evaluate antigen expression of cells cultured on electrospun mats [41]. Results from the study reported by Baiguera *et al.* showed that decellularized brain extracellular matrix (dBECM)-gelatin mats induced a significant ($p<0.05$) decrease in CD54 expression and the higher GFAP expression, suggesting a more effective differentiation potential towards neural (glial) pathway [41].

In vivo Evaluation of Tissue Responses to Biomaterials

The *in vivo* assessment of the compatibility of biomaterials with tissue is a critical element of the development and implementation of implants for human use. While *in vitro* systems yield important fundamental information about certain elements of cellular and molecular interactions with biomaterials, they cannot replace *in vivo* evaluations. *In vivo* testing of a biomaterial often involves sterilization of the material followed by implantation in an animal model. *In vivo* tests listed under the ISO 10993 guidelines include the following: Part 3- tests for genotoxicity, carcinogenicity and reproductive toxicity, Part 4- selection of tests for interaction with blood, Part 6- tests for local effects after implantation, Part 10-tests for irritation and sensitization, and Part 11- tests for systemic toxicity [67].

All materials undergo tissue responses when implanted into living tissues [68]. Fundamental aspects of tissue responses to materials include injury, inflammatory and wound healing responses, foreign body reactions, and fibrous encapsulation of the biomaterial. Studies of the tissue response to implants require a methodology capable of measurements at the molecular, cellular and tissue level. This complex sequence of biological events cannot be simulated *in vitro*, thus, explaining the need for an appropriate model for *in vivo* evaluation of tissue compatibility and device efficacy.

Factors Affecting Cytocompatibility of Electrospun Nanofibers

Major material properties that may influence the host response may be divided into characteristics of the bulk material and those of the surface [69]. These include the following: bulk material composition, micro/nano-structure, morphology, crystallinity, elastic constants, water content, hydrophobic–hydrophilic balance, macro/micro/nano-porosity, surface chemical composition, surface molecular mobility, surface topography, surface energy, surface electrical/electronic properties, degradation profile, degradation product and toxicity, additives, catalysts, contaminants and their toxicity.

Interaction of cells and nanoscaffolds

The complex and dynamic cell-ECM communication takes place through both integrin and non-integrin membrane bound receptors [70] (Figure 3). Initially, cell adhesion to the ECM is induced by multiple, low affinity charge and hydrophobic interactions. The spreading phase of cell adhesion is induced by integrins on the cell surface which bind to specific small peptide fragment sequences on the ECM. This allows cell attachment to the ECM through focal adhesions and promotes direct communication between the two. Integrin binding is specific and reversible. It has been shown that cells behave differently when cultured in 3D compared to traditional 2D cultures. Also, they adopt more *in vivo* like morphologies [71]. The mechanical signalling of cells is altered when cultured in 3D, compared to those in 2D, thereby influencing cell-receptor litigation, intercellular signalling and cellular migration [72-73]. The diffusion

and adhesion of proteins, growth factors and enzymes, which ensures cell viability and functions, are influenced by the 3D environment [73].

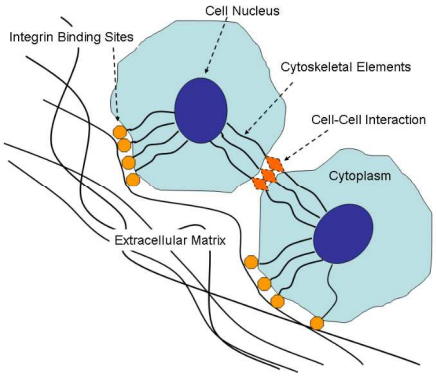

Figure 3: Diagram depicting integrins favoring cell-ECM interaction. Reprinted with permission from [70], S. A. Sell, P. S. Wolfe, K. Garg, J. M. McCool, I. A. Rodriguez and G. L. Bowlin, *Polymers*, 2010, 2(4), 522.

Numerous physico-chemical features of the scaffolds such as fiber diameter, pore size, surface patterning, topography, hydrophilicity, alignment and roughness, are reported to play important roles in cell attachment, proliferation as well as differentiation [74-86].

Fiber diameter and pore size

Cell morphology and viability are influenced by fiber diameter. Indeed, the number of live chondrocytes on smaller diameter electrospun chitosan mat was higher compared to the larger diameter mat [81]. A study by Lowery *et al.* [82] showed that fibroblasts proliferated at a faster rate on scaffolds with pore diameters greater than 6 µm. Moreover, increasing pore size caused fibroblasts to align along single fibers instead of attaching to multiple fibers. Osteoblasts cultured on 2.1 µm diameter PDLA fibers exhibited a higher aspect ratio (contact guidance) compared to the 0.14 µm fiber [83]. In contrast, ALP activity of osteoblasts in PCL nanofibrous scaffolds was remarkably lower than in microfibrous ones [84]. In another study by Sisson *et al.* [85], the authors concluded that osteoblastic MG63 cells could alter their behaviour based on differences in fiber diameters and pore sizes of electrospun gelatin fibers. Indeed, poor migration of MG63 cells was noted in small diameter scaffold (maximum depth of 18 µm), compared to larger diameter scaffold whereby cells penetrated into the scaffold with a maximum depth of 50 µm. MG63 cell differentiation was favoured on small diameter scaffolds compared to large diameter ones at days 3 and 7, but the ALP levels were the same for both scaffold types by day 14. Furthermore, NIH 3T3 fibroblast cell adhesion and growth kinetics on electrospun PCL scaffolds was found to decrease with increasing fiber diameter [86].

Surface patterning & topography

Surface patterning and topography is a key feature influencing the type of cell-nanomaterial interactions [74,75,78]. The effects of surface micro/nano patterning on the modulation of bone cell response are fully discussed in a review by Mitra *et al.* [75]. Following adhesion to a given surface, the cell explores the environment and migrates via nanoscale processes such as filopodia and lamelliopodia. Various research studies conducted in view of investigating the influence of nanoscale features, in particular pattern size and shape, distance between the pattern features, arrangement of the pattern features are detailed. Moreover, mathematical models developed to predict the strength of cellular adhesion on nanorough surfaces are also presented.

Pelipenko *et al.* [78] showed that keratinocytes attached more strongly to the electrospun PVA nanofibers, compared to PVA film. The high surface area of the nanofibers enabled the attachment of a large number of cells, physical entrapment of the cells in the nanofibrillar network as well as multiple focal adhesion points on different nanofibers. Furthermore, in a study by Wang *et al.,* a genipin cross-linked chitosan/nano-HA composite framework (GCFH) was fabricated and compared with genipin cross-linked chitosan framework (GCF) [87]. GCFH enhanced the osteogenic differentiation of rat MSCs in comparison to GCF after incubation in an osteogenic medium for 7 days. It was postulated that the scaffold`s chemical property and nanotopography favoured stem cell proliferation and differentiation in GCFH samples.

Surface roughness

Surface roughness of biomaterials is one of the important parameters that affect cell behavior [76]. Surface roughness may be determined through the use of atomic force microscopy (AFM). The roughness parameter of a given surface, R_a is defined as the centerline average or the distance between the highest and the lowest point of the surface irregularities [88]. Adhesion and proliferation of human umbilical vein endothelial cells (HUVECs) on the PU-PEG_{mix} (R_a= 39.79±10.48) films were more pronounced than that of the PU-PEG_{2000} (R_a= 20.10±7.87). Figure 4 shows the AFM images of the two surfaces with different R_a values. In another study, whereby surface roughness, R_a was measured with a profilometer, the latter was defined as the average value of the distance from the surface to a center reference line [89]. Lampin *et al.* reported that the effect of roughness of PMMA surfaces in enhancing cell adhesion might be due to triggering of sub-confluent cells to secrete extra-cellular proteins which allowed better anchorage of cells to their substratum [90] while others reported that the roughness of the titanium surface could modulate the product of cytokine and growth factor of cells, but reduced cell numbers [91]. Very interestingly, the effect of surface roughness is different for different cell lines. For instance, a study by Xu *et al.* [76] proved that vascular endothelial cell function was enhanced on the smooth solvent-cast surface rather than on the rough electrospun surface of poly(L-lactic acid). On the other hand, hMSCs` proliferation and osteogenic differentiation were enhanced with surface roughness of electrospun PLGA/calcium phosphate cement scaffolds [92].

PU-PEG_{mix}: Different molecular weights or chain lengths of polyethylene glycol (PEG) were mixed and then grafted to a polyurethane (PU) surface

PU-PEG_{2000}: PEG with a molecular weight of 2000 grafted to PU

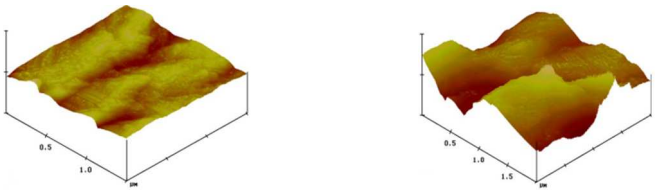

(a) **(b)**

Figure 4: AFM images of (a) PU-PEG_{2000} (R_a= 20.10±7.87) (b) PU-PEG_{mix} (R_a= 39.79±10.48). Adapted with permission from [88], T. W. Chung, D. Z. Liu, S. Y. Wang and S. S.

Wang, *Biomaterials,* 2003, 24(25), 4655-4661. © 2003, Elsevier.

Nanofiber alignment

Several studies have investigated the effects of fiber orientation on cell adhesion, morphology, proliferation and differentiation [74,78,79]. These studies showed that fiber alignment favoured cell growth. Randomly oriented PVA nanofibers were found to limit cell mobility while aligned nanofibers guided keratinocyte cell growth *in vitro* [78]. Furthermore, human osteoblast-like MG63 cells on randomly-oriented PLLA scaffolds showed irregular polygonal forms with no obvious orientations, while on aligned scaffolds, the cells showed polarized forms with orientations along the fiber directions [79] (Figure 5). Wang *et al.* [93] demonstrated that neural progenitor cells (NPCs) grew more efficiently on aligned nanofibers than on substrates with random orientation. Similarly, aligned PLLA nanofibers could enhance the differentiation of bone marrow stromal cells into osteocytes compared to the randomly oriented one [94]. In addition, aligned PCL/PLLA/nano-HA scaffolds increased the differentiation of human unrestricted somatic stem cells (USSCs) into bone cells [95]. This can be explained by the fact that ordered nanomaterials better mimic the orderly pattern of natural ECM in which the fibers are parallel to each other and form an arranged network to support cells [93].

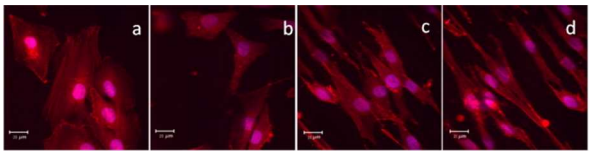

Figure 5: Laser scanning confocal microscopy (LSCM) micrographs of immunostained a-actin filaments in MG63 cells after 1 day of culture. Cell actin (green) and nuclei (red) were stained in cells cultured on (a) TCP; (b) random; (c) parallel-aligned; (d) hyperparallel-aligned scaffolds. Reprinted with permission from [79], B. Wang, Q. Cai, S. Zhang, X. Yang and X. Deng, *J. Mech. Behav. Biomed. Mater,* 2011, 4(4), 600. © 2011, Elsevier.

Fiber composition- wettability

Wettability of electrospun hydrophobic scaffolds may be tailored through introduction of hydrophilic polymers [77,80]. Hydrophilic surfaces have long been recognized to promote cellular growth and improved biocompatibility [80]. Indeed, several studies have shown that cell growth was favoured on less hydrophobic surfaces [96-97]. Recent studies have demonstrated that cells adhere, spread and grow more easily on moderately hydrophilic substrates than on hydrophobic or very hydrophilic ones [98]. Cell culture studies showed that the attachment and proliferation rate of human prostate epithelial cells (HPECs) were improved by introducing PVA into the electrospun PCL mats [77]. In line with this, better human dermal fibroblast cell attachment was observed on PDX/PMeDX scaffolds (increased hydrophilicity) compared to PDX fibrous mat [16]. Moreover, the hydrophilicity of the PDLLA/PEG mats was significantly improved with increasing amount of PEG. HDFs interacted and integrated well with fibers containing 20 and 30% PEG, which provided significantly better environment for biological activities of HDFs than electrospun PDLLA mats [58]. Similarly, human umbilical vein endothelial cells (HUVECs) seeded on the PU/PEG scaffolds were found to attach and proliferate better compared to neat PU scaffold [99].

Cellular response and suitability of electrospun scaffolds

Aforementioned features such as fiber diameter, surface roughness, fiber alignment and wettability influence cell morphology, proliferation and migration. In addition, cell type and nature of polymer also affect the performance of electrospun scaffolds, as summarised in Table 1. For example, better osteoblast growth, with a higher aspect ratio (contact guidance) was noted on larger diameter PDLA fiber compared to smaller diameter ones [83]. On the other hand, this effect was reversed for osteoblasts cultured on electrospun PCL mats. In fact, higher ALP activity was observed on microfibers compared to nanofibers [84]. Although PDLA is a poly(ester), its thermal properties are very different to PCL. PDLA is an amorphous polymer while PCL is semi-crystalline. A study by Asran *et al.* [101], demonstrated that increasing PVA content in electrospun PVA/PHB mats (enhanced wettability) resulted in a decrease in number of viable fibroblasts and enhanced adhesion and proliferation of keratinocytes. This was explained by the strong cell-cell adhesions of keratinocytes which is absent in fibroblasts [103]. Hence, cellular response depends on cell type and nature of scaffold and it is inappropriate to draw general conclusions.

Cytocompatibility Tests on Electrospun Nanofibers

In this section, results of few cytocompatibility studies carried out on electrospun PDX, PCL, PLA, chitosan, collagen and their blends will be summarized. Regardless of the ultimate purpose of the electrospun scaffold for *in vitro* investigations (cell viability, proliferation, differentiation or migration), cell and scaffold handling should be thoroughly described for repeatability purposes [12]. In most articles reporting biological assays, cell type and origin, type of culture medium and passage number are often included. However, crucial details such as scaffold sterilization methods, seeding method etc. are often omitted. Scaffold sterilization methods include ethylene oxide, UV radiation or soaking in ethanol. It is important to analyse the scaffold morphology after sterilization since some sterilization techniques may cause degradation [99,104,105]. Although the initial cell seeding density is often reported, the initial seeding volume and subsequent incubation time for cell attachment is not always mentioned [99]. The method employed to immobilize the scaffold i.e. whether it is in direct contact with a substrate underneath or it is suspended between two rings, also affects the results.

Polyester-Based Nanofibers

Electrospun PCL-based nanofibers

PCL is an aliphatic linear biocompatible and bioresorbable polyester, with a glass transition temperature of 62 °C and a melting point of 55–60 °C [99]. Due to its semi-crystalline and hydrophobic nature, it exhibits a very slow degradation rate (2–4 years depending on the starting molecular weight) and has mechanical properties suitable for a variety of applications [106-108]. It has been approved by the Food and Drug Administration (FDA) and has been clinically used as a slow

release drug delivery device and suture material since the 1980s (i.e. Capronor®, SynBiosys®, Monocryl® suture). A major disadvantage of PCL, however, is its hydrophobic nature, which results in lack of cell attachment and uncontrolled biological interactions with the material [109].

Yoshimoto *et al.* used mesenchymal stem cells (MSCs) derived from the bone marrow of neonatal rats for *in vitro* culture studies for up to 4 weeks on electrospun PCL nanofibers [110]. Cells penetrated in the cell-polymer constructs after 1 week. SEM revealed that the surfaces of the cell-scaffold constructs were covered with cell multilayers at 4 weeks. Furthermore, mineralization and type I collagen were observed at 4 weeks. In another study, Li *et al*. [111] seeded hMSCs onto PCL nanofibrous scaffolds. The cells were induced to differentiate along adipogenic, chondrogenic, or osteogenic lineages by culturing in specific differentiation media. Histological and SEM observations, gene expression analysis and immunohistochemical detection of lineage-specific marker molecules confirmed the formation of 3-D constructs containing cells differentiated into the specified cell types.

Blending and copolymerization have been used to overcome this problem [112-116].

Table 2 summarizes results of *in vitro* cell culture studies carried out on electrospun PCL and PCL-blend nanofibers with natural polymers such as collagen, gelatin, HA, chitin, fucoidan, and synthetic polymers such as PEG. Table 3 gives a summary of *in vivo* studies on electrospun PCL and PCL based nanofibers.

Electrospun PLA-based nanofibers

Poly (lactic acid) (PLA) is the most extensively studied and utilized biodegradable and renewable thermoplastic bio-based polyester. Early studies have investigated the use of PLA as bone plates and screws [150]. A 5-year *in vitro* and *in vivo* study of the biodegradation of polylactide plates showed that the foreign-body reaction was mainly mild and the osteotomies were well united [151].

More recent applications involve the use of electrospun PLA as tissue engineering scaffolds [152-155], in drug delivery applications [156], as suitable bio-absorbable membranes [157], and for suture application [158]. Briefly, braided PLLA nanofibers coated with chitosan could tie wounded tissues for a complete healing without any breakage, had no cellular toxicity and could promote cell growth [158]. The chitosan-coated PLLA sutures showed better histological compatibility than a silk suture in the *in vivo* study.

Table 4 summarizes *in vitro* cytocompatibility studies carried out on electrospun PLA or PLA based nanofibers with HA, tri-calcium phosphate, gelatin and PCL. A summary of *in vivo* results are shown in Table 5.

Poly(ester-ether)-Based Nanofibers

Electrospun PDX nanofibers

PDX is a semi-crystalline (55% crystalline fraction), biodegradable polyester that was originally developed for use as a degradable suture (Ethicon, Inc., a Johnson and Johnson Company) [33]. Electrospinning of PDX was first reported by Boland *et al*. [172] in 2005. The compatibility, degradation rate, and mechanical properties of PDX are of interest in the design of tissue engineering scaffolds. Since then, many papers have been published regarding the use of electrospun PDX blend nanofibers for potential biomedical applications [173-177]. Recently, Kalfa *et al.* used an electrospun PDX valved patch to replace the right ventricular outflow tract (RVOT) in a growing lamb model [178]. Compared with control polytetrafluoroethylene (PTFE)-pericardial patches, tissue-engineered RVOT were neither stenotic nor aneurismal and displayed a growth potential, with less fibrosis, less calcifications and no thrombus. The PDX scaffold was completely degraded within 8 months and replaced by a viable, three-layered, endothelialized tissue and an extracellular matrix with elastic fibers similar to that of native tissue. Hakimi *et al.* evaluated the suitability of PDS sutures for the construction of a patch by measuring cell survival, proliferation and migration of human tendon-derived fibroblasts [179]. The degradable PDSII showed good interaction with human tendon-derived fibroblasts *in vitro*, but relatively poor cell adhesion. Cytocompatibility studies carried out on electrospun PDX demonstrated that tendon derived cells grew very well for up to 21 days and that the degradation products which leached from the patch over 8 weeks were safe with only a minimal effect by the end of the experiment [180]. Cells seeded on the electrospun patch showed good cell attachment, with no visible clumps of cells (Figure 6). Cells appeared elongated along the electrospun fibers whilst forming numerous cell-cell contacts.

Electrospun PDX /natural polymer blends

Preliminary cell culture studies on electrospun PDX/elastin blend nanofibers revealed that cells migrated into the fibrous networks of the blends, while the human dermal fibroblasts (HDFs) remained on the surface of the pure PDX scaffold after 24 hours [173]. Histological examination further confirmed that HDFs penetrated the full thickness of the elastin-containing scaffolds, with no penetration in the case of the pure PDX scaffold after 7 days. PDX/collagen electrospun blends have also been fabricated [181]. Similar results were obtained whereby preliminary *in vitro* cell culture with HDFs demonstrated favourable cellular interactions on PDX/collagen nanofibers, with prominent cell migration into the scaffolds compared to simple surface spreading with no penetration on pure PDX scaffolds.

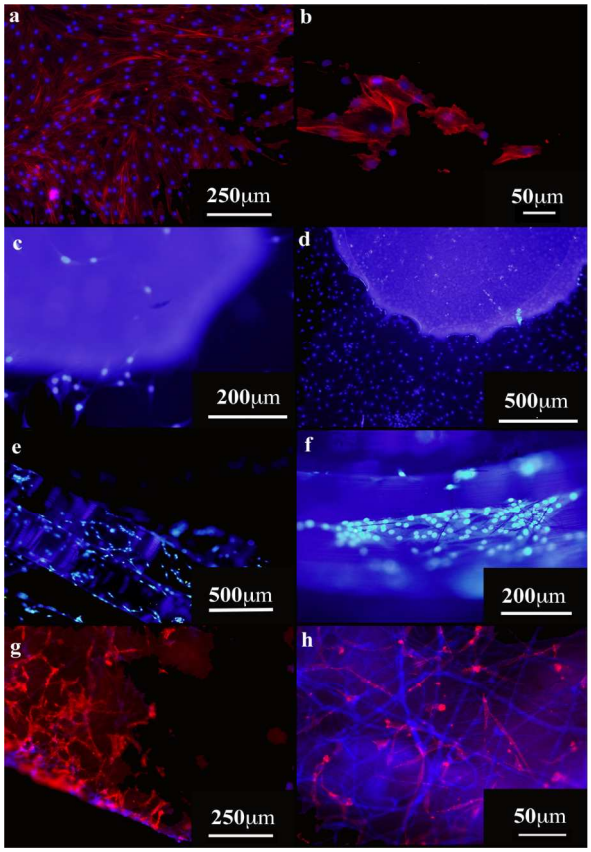

Figure 6: The appearance of human supraspinatus derived cells attached to plastic (a, b), A polydioxanone "drop" (c, d), Polydioxanone sutures (e, f) and the electrospun patch (g, h). Cells were stained with nuclei stain (blue, DAPI) and actin filaments (red, Rhodamine-Phallidin stain, in images a, b, g, and h). Reprinted with permission with [180], O. Hakimi, R. Murphy, U. Stachewicz, S. Hislop and A. J. Carr, *European Cells and Materials,* 2012, 24, 344.

Natural Polymer-Based Nanofibers

Electrospun collagen-based nanofibers

Collagen is a key component of tissue architecture, providing tensile strength and allowing cell-matrix and matrix-matrix interaction [182,33]. Up to now, 28 different types of collagen have been identified, with types I, II, III, V and XI involved in forming fibrillar structures. All collagen molecules have a triple helix structure and have 4-hydroxyproline as distinctive marker. It is an attractive biomaterial for tissue engineering applications given its low antigenicity, low inflammatory and cytotoxic responses, high water affinity, good cell compatibility, availability of various methods of isolation from a variety of sources and biodegradability. Table 6 summarizes the different types of collagen and their body location [183-185].

Table 6: Types of collagen and their locations in the body

Types	Locations
Type I	Bone, skin, dentin, cornea, blood vessels, fibrocartilage and tendon
Type II	Cartilaginous tissues
Type III	Skin, ligaments, blood vessels and internal organs
Type IV	Basement membrane in various tissues
Type V	Blood vessel wall, synovium, corneal stoma, tendon, lung, bone, cartilage and skeletal muscle

Electrospinning of collagen was first reported with the use of poly (ethylene oxide) (PEO) in 2001 [186]. Since then, many papers have been published on this aspect [181,187,188]. Electrospun collagen mats lack mechanical and structural stability upon hydration. Cross-linking with glutaraldehyde vapours, formaldehyde and epoxy compounds has been considered to increase the strength of electrospun collagen mats. However, this leads to an enhanced risk of cytotoxicity and calcification when used *in vivo* [160]. A new technique of imparting desirable mechanical properties and maintaining the nanofibrous structure, while preventing any cytotoxic effects, involves the use of 1-ethyl-3-(3-dimethylaminopropyl) carbodiimide hydrochloride (EDC) in ethanol [160,189]. Carbodiimides have been used to cross-link collagen in gels and in lyophilized native tissue specimens but had not been used for electrospun mats until recently [189]. Another way to improve the mechanical properties is by blending collagen with synthetic polymers [190].

Tables 7 and 8 summarize *in vitro* cell culture and *in vivo* studies on electrospun collagen and collagen-blend nanofibers.

Electrospun elastin-based nanofibers

Elastin is a key structural protein found in the native ECM of connective tissues. It constitutes the walls of arteries and veins, ligaments, lung parenchyma, skin and intestines [202-203]. Elastin is chemically inert, highly insoluble polymer, and is composed of several covalently cross-linked molecules of its precursor, tropoelastin, a 67-kDa soluble, non-glycosylated, highly hydrophobic protein [203-204]. Elastin has become increasingly popular as a biomaterial for various tissue engineering applications, such as skin [205], heart valves [206], and elastic cartilage [207]. When used as a scaffold *in vivo*, soluble elastin exhibits no signs of calcification, a problem with insoluble elastin scaffolds. Soluble elastin scaffolds have also been shown to exert positive biological effects on a variety of cell types, including increasing angiogenesis and elastic fiber synthesis [208]. Nivison-Smith *et al.* electrospun tropoelastin from HFIP, followed by cross-linking to form synthetic elastin microfibrous scaffolds [209]. Cells were found to attach and grow on the seeded surface of the cross-linked scaffolds, with no negative effects from the different cross-linking methods on cell morphology and proliferation.

Tables 9 and 10 gives a summary of *in vitro* and *in vivo* studies conducted on electrospun elastin and elastin blend nanofibers.

General Trend in cellular/tissue response versus polymer/scaffold

Both *in vitro* and *in vivo* data show that cellular and tissue response are scaffold dependent and the latter's performance in general depends on mechanical performance and biocompatibility. For instance, PCL/collagen and PCL/chitin showed better fibroblast infiltration compared to pure PCL scaffold. *In vivo* studies using PCL scaffolds demonstrated good response with blood vessels, bone and neural cells. The combination of polyester/collagen also gave good response with blood vessels. Elastin, on the other hand, caused mild inflammatory skin reaction. PLA scaffolds favoured osteoblast

adhesion, proliferation and growth both *in vitro* and *in vivo*. HA addition to both synthetic and natural polymers provided a favourable environment for bone cells.

Preclinical/ Clinical Applications of Electrospun Nanofibers

Several preclinical studies have been conducted on the use of electrospun fibers for tissue regeneration as summarized in Tables 3, 5, 8 and 10. For example, implantation of electrospun PCL scaffolds into the flexor digitorum profundus tendon of mice hindpaws gave promising results with minimal inflammatory reaction. In addition, cells infiltrated into the scaffold [218].
The Clinical Trials Website [219] was used to check for applications of electrospun nanofibers that are currently being evaluated by a clinical trial. The clinical trials summarised in Table 11 are the result of a search using the terms: electrospinning, nanotechnology, scaffold, electrospun nanofibers. Recently, poly(lactide-*co*-glycolide) biodegradable scaffolds, seeded with neural stem cells have been proposed by InVivo Therapeutics to treat acute spinal cord injuries. The company received approval from FDA for the First Human Trial Using Biomaterials for Traumatic Spinal Cord Injury last year and the trial is now underway [220].

Few electrospun polymeric-based products have been commercialized. For instance, AVflo™, Nicast's CE certified polyurethane vascular access graft was the first one commercialized using electrospun nanofibers and is currently available on the EU market, several Asian countries and Israel [221]. Another product commercialized by the same company is NovaMesh™ which is used in the treatment of ventral hernia [222]. The latter consists of a smooth side and a nanofibrous side which is placed in contact with the tissue. Studies showed improved resistance to tissue adhesion on the visceral-facing surface, with excellent tissue ingrowth on the fascial surface. Several other nanofiber-based products such as NPmimetic, VISION and BIO-DISC are currently under development by Nicast. Furthermore, the CartiGro ACT technique (Stryker, Montreux, Switzerland) uses a collagen I/III based scaffold (Chondro-Gide; Geistlich Biomaterials, Switzerland) onto which cells (CellGenix- Freiburg, Germany) are cultured [223]. This product is marketed for cartilage repair by Stryker in Austria and Germany. Animalclot™ (St. Teresa Medical Inc.,), an electrospun nanofibrous dextran matrix loaded with fibrin producing proteins such as thrombin and fibrinogen is being used in dogs and horses for traumatic bleeding [224]. European regulatory approval for human use is anticipated in mid-2014 and in the United States in early 2016 (Fastclot® and Wrapclot®) [224]. Few more products are available for veterinary use. These include NanoCareV™ scaffolds for surface skin and wound care [225], NanoLigV™ scaffolds to replace and amend ligaments and tendons [226], NanoVesselIV™ synthetic blood vessel for enhancement of vein and artery formation [227] and NanoBoneV™ bone replacement scaffolds for bone regeneration [228]. Each product line is available in a variety of sizes to meet the needs of any animal. Several companies (Cytoweb, eSpin, NanofiberSOLUTIONS™, SNS Nano Fiber Technology, Engineered Fibers Technology) are producing electrospun nanofibrous mats for cell culture research or clinical applications. Mats fabricated from a wide range of polymers with varying molecular weights, copolymer composition, fiber diameter and fiber orientation are available.

Perspectives and Conclusions

As the field of regenerative medicine experiences rapid growth, the development of polymeric-based nanofibers for tissue engineering applications attracts accrued interest. Despite enormous advancements, the best combination of material and nano features still remains unknown. Moreover, a number of hurdles need to be overcome in the translation of scaffolds from lab to clinic. To reach commercial stage, a number of stringent requirements imposed by regulating agencies have to be fulfilled. Another major issue concerns the scaling-up of the manufacturing process such that scaffolds may be fabricated in large quantities with low batch-to-batch variability. Despite the widespread use and the billion-dollar industry producing medical devices and implants, there is still a lack of fundamental understanding of the interlinked reactions that occur when an artificial material is exposed to cells. In that respect, we have summarized in this review the status of cytocompatibility and cytotoxicity studies of a range of electrospun nanofibers based on poly(esters), poly(ester-ether), natural polymers and blends of natural/synthetic polymers that are currently being investigated in different fields of tissue engineering. While the majority of *in vitro* tests have demonstrated that a range of electrospun nanofibers showed no toxicity and inflammatory response towards living cells, the optimized fiber diameter or inter-fiber diameter for cell growth and migration remains a challenge to be addressed. *In vivo* testing of electrospun nanofibers are very few in comparison to *in vitro* tests. *In vivo* evaluation of biomaterials correlated with factors affecting their cellular responses such as surface roughness, fiber alignment, fiber composition has been discussed. The use of electrospun nanofibers at clinical level is still embryonic as a number of issues such as animal use concerns, lack of reliable correlations between *in vitro-in vivo* experiments, analytical or technical limitations and high cost.

Acknowledgements

We thank the Tertiary Education Commission (Mauritius) for awarding a PhD scholarship to N. Goonoo. We are grateful to the Mauritius Research Council (Mauritius) for supporting biomaterials and drug delivery research at the ANDI Centre of Excellence for Biomedical and Biomaterials Research (CBBR). We are also most indebted to our close collaborator, Prof. Gary Bowlin at the University of Memphis, for his continuous support.

Notes and References

[a]ANDI Centre of Excellence for Biomedical and Biomaterials Research, MSIRI Building, University of Mauritius, Réduit, Mauritius; * Corresponding author; E-mail: djhurry@uom.ac.mu

1. M. T. Hunley and T. E. Long, *Polymer International*, 2008, **57**, 385.
2. J. Doshi and D. H. Reneker, *Journal of Electrostatics*, 1995, **35(2-3)**, 151.
3. J. Zeng, X. Xu, X. Chen, Q. Liang, X. Bian, L. Yang and X. Jing, *Journal of Controlled Release*, 2003, **92(3)**, 227.

4. T. J. Sill and H. A. Von Recum, *Biomaterials*, 2008, **29(13)**, 1989.
5. Z. M. Huang, Y. Z. Zhang, M. Kotaki and S. Ramakrishna, *Composites Science and Technology*, 2003, **63**, 2223.
6. R. Gopal, S. Kaur, Z. Ma, C. Chan, S. Ramakrishna and T. Matsuura, *Journal of Membrane Science*, 2006, **281**, 581.
7. J. Xie, X. Li and Y. Xia, *Macromolecular Rapid Communication*, 2008, **29(22)**, 1775.
8. L. Zhang and T. J. Webster, *Nano Today*, 2009, **4**, 66.
9. D. R. Nisbet, J. S. Forsythe, W. Shen, D. I. Finkelstein and M. K. Horne, *Journal of Biomaterial Applications*, 2009, **24(1)**, 7.
10. E. K. F. Yim and K. W. Leong, *Nanomedicine, Nanotechnology, Biology and Medicine*, 2005, **1(1)**, 10.
11. Z. Ma, M. Kotaki, R. Inai and S. Ramakrishna, *Tissue Engineering*, 2005, **11(1/2)**, 101.
12. A. Cipitria, A. Skelton, T. R. Dargaville, P. D. Dalton and D. W. Hutmacher, *Journal of Material Chemistry,* 2011, **21**, 9419.
13. C. Zhao, A. Tan, G. Pastorin and H. K. Ho, *Biotechnology Advances*, 2013, **31**, 654.
14. S. Martino, F. D`Angelo, I. Armentano, J. M. Kenny and A. Orlacchio, *Biotechnology Advances*, 2012, **30**, 338.
15. N. Goonoo, A. Bhaw-Luximon, G. L. Bowlin and D. Jhurry, *Polymer International*, 2013, **62(4)**, 523.
16. N. Goonoo, A. Bhaw-Luximon, I. A. Rodriguez, D. Wesner, H. Schönherr, G. L. Bowlin and Dhanjay Jhurry, *Biomaterials Science*, 2014, **2**, 339.
17. S. Miyamoto, B. Z. Katz, R. M. Lafrenie and K. M. Yamada, *Annals of New York Academy of Sciences,* 1998, **857**, 119.
18. A. L. Berrier and K. M. Yamada, *Journal of Cellular Physiology,* 2007, **213(3)**, 565.
19. J. Halper and M. Kjaer, *Advances in Experimental Medicine and Biology,* 2014, **802**, 31.
20. S. Schlie-Wolter A. Ngezahayo and B. N. Chichkov, *Experimental Cell Research*, 2013, **319(10)**, 1553.
20.
21. Biodegradable Systems in Tissue Engineering & Regenerative Medicine, 2004, Edited by Rui L. Reis, Julio San Roman.
22. D. S. Kohane, M. Lipp, R. C. Kinney, D. C. Anthony, D. N. Louis, N. Lotan and R. Langer, *Journal of Biomedical Materials Research Part A*, 2002, **59**, 450.
23. J. M. Anderson, *European Journal of Pharmaceutics and Biopharmaceutics,* 1994, **40**, 1.
24. H. Epstein-Barash, I. Shichor, A. H. Kwon, S. Hall, M. W. Lawlor, R. Langer and D. S. Kohane, *Proc. Natl. Acad. Sci. U.S.A,* 2009, **106**, 7125.
25. S. P. Hudson, R. F. Padera, R. Langer and D. S. Kohane, *Biomaterials*, 2008, **29**, 4045.
26. D. S. Kohane, N. Plesnila, S. S. Thomas, D. Le, R. Langer and M. A. Moskowitz, *Brain Research*. 2002, **946**, 206.
27. M. Goldberg, R. Langer and X. Jia, *Journal of Biomaterials Science., Polymer Edition,* 2007, **18**, 241.
28. N. Lewinski, V. Colvin, R. Drezek, *Small*, 2008, **4(1)**, 26.
29. T. F. Slater, B. Sawyer and U. Straeuli, *Biochimica et Biophysica Acta,* 1963, **77**, 383.
30. S. K. Bhatia and A. B. Yetter, *Cell Biology and Toxicology,* 2008, **24**, 315.
31. H. K. Makadia and S. J. Siegel, *Polymers*, 2011, **3**, 1377.
32. P. A. Madurantakam, I. A. Rodriguez, C. P. Cost, R. Viswanathan, D. G. Simpson, M. J. Beckman, P. C. Moon and G. L. Bowlin, *Biomaterials*, 2009, **30(29)**, 5456.
33. C. P. Barnes, S. A. Sell, E. D. Boland, D. G. Simpson and G. L. Bowlin, *Advanced Drug Delivery Reviews*, 2007, **59**, 1413.
34. M. S. Schoichet, *Macromolecules,* 2010, **43**, 581.
35. B. N. Brown, J. E. Valentin, A. M. Stewart-Akers, G. P. McCabe and S. F. Badylak, *Biomaterials*, 2009, **30**, 1482.
36. M. Zhang, Biocompatibility of materials. In: Shi D, editor. Biomaterials and Tissue Engineering, Heidelberg: Springers; 2003. p 83–137.
37. An Introduction to Biomaterials, Second Edition, Ed Jeffrey O. Hollinger, pg 64
38. D. F. Williams, *Biomaterials*, 2008, **29**, 2941.
39. C. F. Jones and D. W. Grainger, *Advanced Drug Delivery Reviews*, 2009, **61**, 438.
40. Biomaterials Science, An Introduction to Materials In Medicine, Edited by B. Ratner & A. Hoffman, chap 5
41. S. Baiguera, C. Del Claudio, E. Lucatelli, E. Kuevda, M. Boieri, B. Mazzanti, A. Bianco and P. Macchiarini, *Biomaterials*, 2014, **35**, 1205.
42. J. Rnjak-Kovacina, S. G. Wise, Z. Li, P. K. M. Maitz, C. J. Young, Y. Wang and A. S. Weiss, *Acta Biomaterialia*, 2012, **8**, 3714.
43. J. Xue, B. Feng, R. Zheng, Y. Lu, G. Zhou, W. Liu, Y. Cao, Y. Zhang and W. J. Zhang, *Biomaterials*, 2013, **34**, 2624.
44. S. G. Kumbar, S. P. Nukavarapu, R. James, L. S. Nair and C. T. Laurencin, *Biomaterials,* 2008, **29**, 4100.
45. E. I. Paşcu, J. Stokes and G. B. McGuinness, *Materials Science and Engineering C*, 2013, **33**, 4905.
46. R. Moore, I. MacCoubrey and R. Haugland, *Journal of Cellular Biology,* 1990, **111**, 58 A.
47. S. J. Lee, J. J. Yoo, G. J. Lim, A. Atala and J. Stitzel, *Journal of Biomedical Materials Research A,* 2007, **83(4)**, 999.
48. L. Li, G. Yang, J. Li, S. Ding and S. Zhou, *Materials Science and Engineering C* 2014, **34**, 252.
49. J. O'Brien, I. Wilson, T. Orton and F. Pognan, *European Journal of Biochemistrym* 2000, **267**, 5421.
50. G. Haslam, D. Wyatt and P. A. Kitos, *Cytotechnology*, 2000, **32(1)**, 63.
51. P. Brun, F. Ghezzo, M. Roso, R. Danesin, G. Palù, A. Bagno, M. Modesti, I. Castagliuolo and M. Dettin, *Acta Biomaterialia*, 2011, **7**, 2526.
52. J. J Chang, Y. H. Lee, M. H. Wu, M. C. Yang and C. T. Chien, *Carbohydrate Polymers*, 2012, **88**, 1304.
53. R. Chen, C. Huang, Q. Ke, C. He, H. Wang and X. Mo, *Colloids and Surfaces B: Biointerfaces*, 2010, **79**, 315.
54. S. H. Chen, Y. Chang, K. R. Lee and J. Y. Lai, *Journal of Membrane Science,* 2014, **450**, 224.
55. B. Liu, F. Xu, M. Y. Guo, S. F. Cheng, J. Wang and B. Zhang, *Surface & Coatings Technology*, 2013, **228**, S568.
56. G. Ma, D. Fang, Y. Liu, X. Zhu and J. Nie, *Carbohydrate Polymers,* 2012, **87(1)**, 737.
57. Z. X. Meng, H. F. Li, Z. Z. Sun, W. Zheng and Y. F. Zheng, *Materials Science and Engineering C*, 2013, **33**, 699.
58. W. Cui, X. Zhu, Y. Yang, X. Li and Y. Jin, *Materials Science and Engineering C,* 2009, **29**, 1869.
59. Y. Zhang, J. R. Venugopal, A. El-Turki, S. Ramakrishna, B. Su and C. T. Lim, *Biomaterials*, 2008, **29**, 4314.
60. H. Chen, J. Huang, J. Yu, S. Liu and P. Gu, *International Journal of Biological Macromolecules*, 2011, **48**, 13.
61. G. Malich, B. Markovic and C. Winder, *Toxicology* 1997, **124**, 179.
62. H. Tominaga, M. Ishiyama, F. Ohseto, K. Sasamoto, T. Hanamoto, K. Suzuki and M. Watanabe, *Analytical Communications,* 1999, **36**, 47.

63. Y. M. Ju, J. S. Choi, A. Atala, J. J. Yoo and S. J. Lee, *Biomaterials*, 2010, **31**, 4313.
64. K. Ley, Physiology of inflammation. Oxford University Press, New York 2001.
65. C. Dinarello, *Chest,* 2000, **188**, 503.
66. N. Favre, G. Bordmann and W. Rudin, *Journal of Immunological Methods,* 1997, **204**, 57.
67. Cellular Response to Biomaterials edited by L Di Silvio
68. J. M. Anderson, *Annual Review of Material Research,* 2001, **31**, 81.
69. D.F. Williams, *Biomaterials*, 2008, **29**, 2941.
70. S. A. Sell, P. S. Wolfe, K. Garg, J. M. McCool, I. A. Rodriguez and G. L. Bowlin, *Polymers*, 2010, **2(4),** 522.
71. D. R. Nisbet, S. Pattanawong, N. E. Ritchie, W. Shen, D. I. Finkelstein, M. K. Horne and J. S. Forsythe, *Journal of Neural Engineering,* 2007, **4**, 35.
72. B. Knight, C. Laukaitis, N. Akhtar, N. A. Hotchin, M. Edlund and A. R. Horwitz*, Current Biology*, 2000, **10**, 576.
73. L. G. Griffith and M. A. Swartz, *Nature Reviews: Molecular Cell Biology,* 2006, **7**, 211.
74. C. Zhao, A. Tan, G. Pastorin and H. K. Ho, *Biotechnology Advances,* 2013, **31**, 654.
75. J. Mitra, G. Tripathi, A. Sharma and B. Basu, *RSC Adv,* 2013, **3,** 11073.
76. C. Xu, F. Yang, S. Wang and S. Ramakrishna, *Journal of Biomedical Materials Research Part A*, 2004, **71A(1)**, 154.
77. C. H. Kim, M. S. Khil, H. Y. Kim, H. U. Lee and K. Y. Jahng, *Journal of Biomedical Materials Research Part B: Applied Biomaterials* 2006, **78B(2)**, 283.
78. J. Pelipenko, P. Kocbek, B. Govedarica, R. Rošic, S. Baumgartner and J. Kristl, *European Journal of Pharmaceutics and Biopharmaceutics,* 2013, **84(2)**, 401.
79. B. Wang, Q. Cai, S. Zhang, X. Yang and X. Deng, *J. Mech. Behav. Biomed. Mater,* 2011, **4(4)**, 600.
80. B. Veleirinho, F. V. Berti, P. F. Dias, M. Maraschin, R. M. Ribeiro-do-Valle and J. A. Lopes-da-Silva, *Materials Science and Engineering: C,* 2013, **33(1)**, 37.
81. S. E. Noriega, G. I. Hasanova, M. J. Schneider, G. F. Larsen and A. Subramanian, *Cells Tissues Organs*. 2012, **195(3)**,207.
82. J. L. Lowery, N. Datta, G. C. Rutledge, *Biomaterials*, 2010, **31(3)**, 491.
83. A. S. Badami, M. R. Kreke, M. S. Thompson, J. S. Riffle and A. S. Goldstein, *Biomaterial*s, 2006, **27(4),** 596.
84. T. T. Li, k. Ebert, J. Vogel and T. Groth, *Progress in Biomaterials,* 2013, **2**,13
85. K. Sisson, C. Zhang, M. C. Farach- Carson, D. Bruce Chase and J. F. Rabolt, *Journal of Biomedical Materials Research Part A,* 2010, 94A(4), 1312.
86. M. Chen, P. K. Patra, S. B. Warner and S. Bhowmick, *Tissue Engineering*, 2007, **13(3)**, 579.
87. G. Wang, L. Zheng, H. Zhao, J. Miao, C. Sun, N. Ren, J. Wang, H. Liu and X. Tao, *Tissue Engineering Part A*, 2011b, **17**, 1341.
88. T. W. Chung, D. Z. Liu, S. Y. Wang and S. S. Wang, *Biomaterials,* 2003, **24(25)**, 4655.
89. N. Hallab, K. Bundy, K. O'Connor, R. Clark, and R. L. Moses, Proceedings 14th Southern Biomedical Engineering Conference, Shreveport, LA, pp. 81–84, 1995.
90. M. Lampin, R. Warocquier-clerout, C. Legris, M. Degrange, M. F. Sigot-Luizard, *Journal of Biomedical Materials Research,* 1997, **36**, 99.
91. K. Kieswetter, Z. Schwartz, T. W. Hummert, D. L. Cocharn, J. Simpson, D. D. Dean and B. D. Boyan, *Journal of Biomedical Materials Research,* 1996, **32**, 55.
92. C. Bao, W. Chen, M. D. Weir, W. Thein-Han and H. H. Xu, *Acta Biomaterialia,* 2011, **7**, 4037.
93. Y. Wang, M. Yao, J. Zhou, W. Zheng, C. Zhou, D. Dong D, Y. Liu, Z. Teng, Y. Jiang, G. Wei and X. Cui, *Biomaterials,* 2011, **32**, 6737.
94. J. Ma, X. He and E. Jabbari, *Annals of Biomedical Engineering,* 2011, **39**, 14.
95. B. Bakhshandeh, M. Soleimani, N. Ghaemi and I. Shabani, *Acta Pharmacologica Sinica,* 2011, **32**, 626.
96. E. Biazar, M. Heidari, A. Asefnezhad and N. Montazeri, *International Journal of Nanomedicine,* 2011, **6**, 631.
97. C. H. Kim, M. S. Khil, H. Y. Kim, H. U. Lee and K. Y. Jahng, *Journal of Biomedical Materials Research*, 2006, **78**, 283.
98. Y. Arima and H. Iwata, *Biomaterials*, 2007, **28**, 3074.
99. H. Wang, Y. Feng, Z. Fang, W. Yuan and M. Khan, *Materials Science and Engineering C*, 2012, **32**, 2306.
100. A. C. Areis, C. Ribeiro, V. Sencadas, N. Garcia-Giralt, A. Diez-Perez, J. L. Gomez-Ribelles and S. Lanceros-Mendez, *Soft Matter,* 2012, **8**, 5818.
101. A. S. Asran, K. Razghandi, N. Aggarwal, G. H. Michler and T, Groth*, Biomacromolecules*, 2010, **11(12),** 3413.
102. H. K. Noh, S. W. Lee, J. M. Kim, J. E. Oh, K. H. Kim, C. P. Chung, S. C. Choi, W. H. Park and B. M. Min, *Biomaterials,* 2006, **27(21),** 3934.
103. Q. Ren, C. Kari, M. R. D. Quadros, R. Burd, P. McCue, A. P. Dicker and U. Rodeck, *Cancer Research*, 2006, **66**, 5209.
104. W. J. Li, R. Tuli, C. Okafor, A. Derfoul, K. G. Danielson, D. J. Hall and R. S. Tuan, *Biomaterials*, 2005, **26**, 599.
105. H. M. Powell and S. T. Boyce, *Tissue Engineering A,* 2009, **15(8)**, 2177.
106. I. Engelberg and J. Kohn, *Biomaterials*, 1991, **12**, 292.
107. J. C. Middleton and A. J. Tipton, *Biomaterials,* 2000, **21(23)**, 2335.
108. L. S. Nair and C. T. Laurencin, *Progress in Polymer Science*, 2007, **32**, 762.
109. E. S. Place, J. H. George, C. K. Williams, M. M. Stevens, *Chemical Society Reviews,* 2009, **38**, 1139.
110. H. Yoshimoto, Y. M. Shin, H. Terai and J. P. Vacanti, *Biomaterials,* 2003, **24**, 2077.
111. W. J. Li, R. Tuli, X. Huang, P. Laquerriere and R. S. Tuan, *Biomaterials,* 2005, **26**, 5158.
112. Z. C. C. Chen, A. K. Ekaputra, K. Gauthaman, P. G. Adaikan, H. Yu and D. W. Hutmacher, *Journal of Biomaterials Science, Polymer Edition,* 2008, **19(5)**, 693.
113. J. Venugopal, T. Y. L. L. Ma and S. Ramakrishna, *Cell Biology International,* 2005, **29**, 861.
114. Y. C. Lim, J. Johnson, Z. Fei, Y. Wu, D. F. Farson, J. J. Lannutti, H. W. Choi and L. J. Lee, *Biotechnology and Bioengineering,* 2011, **108(1)**, 116.
115. X. Yang, F. Yang, X. F. Walboomers, Z. Bian, M. Fan and J. A. Jansen, *Journal of Biomedical Materials Research, Part A,* 2010, **93(1)**, 247.
116. G. Liao, K. Jiang, S. Jiang and H. Xia, *Journal of Macromolecular Science Part A*, 47, **11**, 1116.
117. W. J. Li, K. G. Danielson, P. G. Alexander and R. S. Tuan, *Journal of Biomedical Materials Research,* 2003, **67(4),** 1105.
118. M. Shin, O. Ishii, T. Sueda and J. P. Vacanti, *Biomaterials,* 2004, **25(17)**, 3717.
119. O. Ishii, M. Shin, T. Sueda and J. P. Vacanti, *The Journal of Thoracic and Cardiovascular Surgery,* 2005, **130(5)**, 1358.

120. W. J. Li, R. Tuli, C. Okafor, A. Derfoul, K. G. Danielson, D. J. Hall and R. S. Tuan, *Biomaterials*, 2005, **26,** 599.
121. W. J. Li, R. L. Mauck, J. A. Cooper, X. Yuan and R. S. Tuan, *Journal of Biomechanics,* 2007, **40**, 1686.
122. D. R. Nisbet, L. M. Y. Yu, T. Zahir, J. S. Forsythe and M. S. Shoichet, *Journal of Biomaterials Science, Polymer Edition,* 2008, **19(5)**, 623.
123. J. Venugopal, T. Y. L. L. Ma and S. Ramakrishna, *Cell Biology International*, 2005, **29**, 861.
124. J. R. Venugopal, Y. Zhang and S. Ramakrishna, *Artificial Organs,* 2006, **30(6)**, 440.
125. S. Srouji, T. Kizhner, E. Suss-Tobi, E. Livne and E. Zussman, *Journal of Materials Science: Materials in Medicine,* 2008, **19**, 1249.
126. J. S. Choi, S. J. Lee, G. J. Christ, A. Atala, J. J. Yoo, *Biomaterials*, 2008, **29(19)**, 2899.
127. X. Yang, J. D. Shah and H. Wang, *Tissue Engineering A,* 2009, **15(4),** 945.
128. Y. M. Ju, J. S. Choi, A. Atala, J. J. Yoo, S. J. Lee, *Biomaterials,* 2010, **31(15)**, 4313.
129. Y. Zhang, H. Ouyang, C. T. Lim, S. Ramakrishna and Z. M. Huang, *Journal of Biomedical Materials Research*, 2005, **72(1)**, 156.
130. Z. Ma, W. He, T. Yong and S. Ramakrishna, *Tissue Engineering,* 2005, **11(7/8)**, 1149.
131. E. J. Chong, T. T. Phan, I. J. Lim, Y. Z. Zhang, B. H. Bay, S. Ramakrishna and C. T. Lim, *Acta Biomaterialia,* 2007, **3**, 321.
132. R. S. Tigli, N. M. Kazaroğlu, I. S. B. Mav, I. O. M. Gümüşderel, *Journal of Biomaterial Science, Polymer Edition*, 2011, **22(1–3),** 207.
133. S. Gautam, A. K. Dinda and N. C. Mishra, *Materials Science and Engineering C*, 2013, **33**, 1228.
134. Y. C. Lim, J. Johnson, Z. Fei, Y. Wu, D. F. Farson, J. J. Lannutti, H. W. Choi and L. J. Lee, *Biotechnology and Bioengineering*, 2011, **108(1)**, 116.
135. A. Bianco, E. Di Federico, I. Moscatelli, A. Camaioni, I. Armentano, L. Campagnolo, M. Dottori, Josè M. Kenny, G. Siracusa and G. Gusmano, *Materials Science and Engineering C,* 2009, **29**, 2063.
136. J. P. Chen and Y. S. Chang, *Colloids and Surfaces B: Biointerfaces*, 2011, **86**, 169.
137. Y. Ji, K. Liang, X. Shen and G. L. Bowlin, *Carbohydrate Polymers,* 2014, **101**, 68.
138. J. S. Lee, G. H. Jin, M. G. Yeo, C. H. Jang, H. Lee, G. H. Kim, *Carbohydrate Polymers,* 2012, **90,** 181.
139. M. Shin, H. Yoshimoto and J. P. Vacanti, *Tissue Eng.,* 2004, **10(1/2)**, 33.
140. B. Nottelet, E. Pektok, D. Mandracchia ,J. C. Tille, B. Walpoth, R. Gurny and M. Möller, *Journal of Biomedical Materials Research, Part A,* 2009, **89(4),** 865.
141. E. Pektok, B. Nottelet, J. C. Tille, R. Gurny, A. Kalangos, M. Moeller, B. H. Walpoth, *Circulation,* 2008, **118(24)**, 2563.
142. E. Piskin, I. A. Işoğlu, N. Bölgen, I. Vargel, S. Griffiths, T. Cavuşoğlu, P. Korkusuz, E. Güzel, S. Cartmell, *Journal of Biomedical Materials Research, Part A,* 2009, **90(4)**, 1137.
143. D. R. Nisbet, A. E. Rodda, M. K. Horne, J. S. Forsythe and D. I. Finkelstein, *Biomaterials*, 2009, **30(27)**, 4573.
144. H. Q. Cao, K. McHugh, S. Y. Chew, J. M. Anderson, *Journal of Biomedical Materials Research, Part A,* 2010, **93(3),** 1151.
145. B. S. Jha, R. J. Colello, J. R. Bowman, S. A. Sell, K. D. Lee, J. W. Bigbee, G. L. Bowlin, W. N. Chow, B. E. Mathern and D. G. Simpson, *Acta Biomaterialia,* 2011, **7(1)**, 203.
146. W. J. Li, H. Chiang, T. F. Kuo, H. S. Lee, C. C. Jiang and R. S. Tuan, *Journal of Tissue Engineering and Regenerative Medicine,* 2009, **3**, 1.
147. Z. C. Chen, A. K. Ekaputra, K. Gauthaman, P. G. Adaikan, H. Yu and D. W. Hutmacher, *Journal of Biomaterials Science, Polymer Edition,* 2008, **19(5)**, 693.
148. B. W. Tillman, S. K. Yazdani, S. J. Lee, R. L. Geary, A. Atala and J. J. Yoo, *Biomaterials,* 2009, **30(4)**, 583.
149. S. Fu, P. Ni, B. Wang, B. Chu, J. Peng, L. Zheng, X. Zhao, F. Luo, Y. Wei, Z. Qian, *Biomaterials,* 2012, **33**, 8363.
150. J. E. Bergsma, W. C. de Bruijn, F. R. Rozema, R. R. Bos and G. Boering, *Biomaterials*, 1995, **16(1)**, 25.
151. R. Suuronen, T. Pohjonen, J. Hietanen and C. Lindqvist, *Journal of Oral and Maxillofacial Surgery*, 1998, *56(5)*, 604.
152. Z. Ma, C. Gao, Y. Gong and J. Shen, *Biomaterials,* 2005, **26**, 1253.
153. F. Yang, R. Murugan, S. Ramakrishna, X. Wang, Y. Ma and S. Wang, *Biomaterials*, 2004, **25**, 1891.
154. H. C. Liu, I. Lee, J. H. Wang, S. H. Yang and T. H. Young, *Biomaterials,* 2004, **25**, 4047.
155. J. P. Chen and C. H. Su, *Acta Biomaterialia,* 2011, **7**, 234.
156. C. He, Z. Huang, X. Han, L. Liu, H. Zhang and L. Chen, *Journal of Macromolecular Science: Physics,* 2006, **45,** 515.
157. X. Zong, K. Kim, D. Fang, S. Ran, B. Hsiao and B. Chu, *Polymer*, 2002, **43**, 4403.
158. W. Hu and Z. M. Huang, *Polymer International*, 2010, **59,** 92.
159. H. Lee, S. Ahn, H. Choi, D. Cho and G. Kim, *Journal of Material Chemistry B*, 2013, **1**, 3670.
160. L. Ylä-Outinen, C. Mariani, H. Skottman, R. Suuronen, A. Harlin, S. Narkilahti, *The Open Tissue Engineering and Regenerative Medicine Journal*, 2010, **3**, 1.
161. X. Xin, M. Hussain and J. J. Mao, *Biomaterials*, 2007, **28**, 316.
162. F. Peng, X. Yu and M. Wei, *Acta Biomaterialia*, 2011, **7(6)**, 2585–2.
163. M. P. Prabhakaran, J. Venugopal and S. Ramakrishna, *Acta Biomaterialia*, 2009**, 5**, 2884.
164. G. Sui, X. Yang, F. Mei, X. Hu, G. Chen, X. Deng and S. Ryu, *Journal of Biomedical Materials Research A.,* 2007, **82(2)**, 445.
165. S. D. McCullen, Y. Zhu, S. H. Bernacki, R. J. Narayan, B. Pourdeyhimi, R. E. Gorga, E. G. Loboa, *Biomedical Materials,* 2009, **4**, 035002 doi:10.1088/1748-6041/4/3/035002.
166. S. Y. Gu, Z. M. Wang, J. Ren and C. Y. Zhang, *Materials Science and Engineering C*, 2009, **29**, 1822.
167. P. Torricelli, M. Gioffre, A. Fiorani, S. Panzavolta, C. Gualandi, M. Fini, M. L. Focarete and A. Bigi, *Materials Science and Engineering C*, 2014, **36**, 130.
168. L. Chen, Y. Bai, G. Liao, E. Peng, B. Wu, Y. Wang, X. Zeng and X. Xie, *PLoS One,* 2013, **8(8)**, 71265.
169. X. M. Mo, C. Y. Xu, M. Kotaki and S. Ramakrishna, *Biomaterials*, 2004, **25(10)**, 1883.

170. L. Lao, Y. Wang, Y. Zhu, Y. Zhang, C. Gao, *Journal of Materials Science: Materials in Medicine,* 2011, **22(8)**, 1873.
171. M. D. Schofer, P. P. Roessler, J. Schaefer, C. Theisen, S. Schlimme, J. T. Heverhagen, M. Voelker, R. Dersch, S. Agarwal, S. Fuchs-Winkelmann and J. R. Paletta, *PLoS One,* 2011, **6(9)**, e25462.
172. E. D. Boland, B. D. Coleman, C. P. Barnes, D. G. Simpson, G. E. Wnek, and G. L. Bowlin, *Acta Biomaterialia,* 2005, **1**, 115.
173. S. A. Sell, M. J. McClure, C. P. Barnes, D. C. Knapp, B. H. Walpoth, D. G. Simpson and G. L. Bowlin, *Biomedical Materials,* 2006, **1**, 72.
174. M. J. McClure, S. A. Sell, D. G. Simpson and G. L. Bowlin, *Journal of Engineered Fibers and Fabrics*, 2009, **4(2),** 18.
175. M. J. McClure, S. A. Sell, C. P Barnes, W. C. Bowen and G. L. Bowlin, *Journal of Engineered Fibers and Fabrics*, 2008, **3(1),** 1.
176. I. A. Rodriguez, P. A. Madurantakam, J. M. McCool, S. A. Sell, H. Yang, P. C. Moon, and Gary L. Bowlin, *International Journal of Biomaterials,* 2012, Article ID 159484, 12 pages.
177. M. J. Smith, K. L. White, D. C. Smith and G. L. Bowlin, *Biomaterials,* 2009, **30(2)**, 149.
178. D. Kalfa, A. Bel, A. Chen-Tournoux, A. Della Martina, P. Rochereau, C. Coz, V. Bellamy, M. Bensalah, V. Vanneaux, S. Lecourt, E. Mousseaux, P. Bruneval, J. Larghero and P. Menasché, *Biomaterials,* 2010, **31,** 4056.
179. O. Hakimi, S. Chaudhury, R. Murphy and A. Carr, *Journal of Biomedical Materials Research B Applied Biomaterials,* 2012, **100(3)**, 685.
180. O. Hakimi, R. Murphy, U. Stachewicz, S. Hislop and A. J. Carr, *European Cells and Materials*, 2012, **24**, 344.
181. C. P. Barnes, S. A. Sell, D. C. Knapp, B. H. Walpoth, D. D. Brand and G. L. Bowlin, *International Journal of Electrospun Nanofiber. Applications,* 2007, **1**, 73.
182. S. A. Sell, P. S. Wolfe, K. Garg, J. M. McCool, I. A. Rodriguez and G. L. Bowlin, *Polymers* 2010, **2**, 522.
183. M. C. Farach-Carson, R. C. Wagner and K. L. Kiick, Extracellular matrix: Structure, function, and applications to tissue engineering. In Tissue Engineering; Fisher, J.P., Mikos, A.G., Bronzino, J.D., Eds.; CRC Press: Boca Raton, FL, USA, 2007; pp. 3-1-3-22.
184. S. Sell, C. Barnes, M. Smith, M. McClure, P. Madurantakam, J. Grant, M. McManus and G. Bowlin, *Polymer International,* 2007, **56**, 1349.
185. S. A. Sell, M. J. McClure, K. Garg, P. S. Wolfe and G. L. Bowlin, *Advanced Drug Delivery Reviews,* 2009, **61**, 1007.
186. L. Huang, K. Nagapudi, R. P. Apkarian, E. L. Chaikof*, Journal of Biomaterials Science Polymer Edition*, 2001, **12,** 979.
187. J. A. Matthews, G. E. Wnek, D. G. Simpson and G. L. Bowlin, *Biomacromolecules,* 2002, **3**, 232.
188. J. A. Matthews, E. D. Boland, G. E. Wnek, D. G. Simpson and G. L. Bowlin, *Journal of Bioactive and Compatible Polymers,* 2003, **18**, 125.
189. C. P. Barnes, C. W. Pemble, D. D. Brand, D. G. Simpson and G. L. Bowlin, *Tissue Engineering,* 2007, **13,** 1593.
190. S. A. Sell, M. J. McClure, K. Garg, P. S. Wolfe and G. L. Bowlin, *Advanced Drug Delivery Reviews*, 2009, **61**, 1007.
191. J. A. Matthews, G. E. Wnek, D. G. Simpson and G. L. Bowlin, *Biomacromolecules*, 2002, **3(2)**, 232.
192. K. J. Shields, M. J. Beckman, G. L. Bowlin and J. S. Wayne, *Tissue Engineering,* 2004, **10(9-10)**, 1510.
193. K. S. Rho, L. Jeong, G. Lee, B. M. Seo, Y. J. Park, S. D. Hong, S. Roh, J. J. Cho, W. H. Park, B. M. Min, *Biomaterials*, 2006, **27(8)**, 1452.
194. S. Zhong, W. E. Teo, X. Zhu, R. W. Beuerman, S. Ramakrishna and L. Y. Yung, *Journal of Biomedical Materials Research Part A,* 2006, **79A(3)**, 456.
195. Y. R. Shih, C. N. Chen, S. W. Tsai, Y. J. Wang and O. K. Lee, *Stem Cells.* 2006, **24(11)**, 2391.
196. S. P. Zhong, W. E. Teo, X. Zhu, R. Beuerman, S. Ramakrishna, L. Yue and L. Yung, *Materials Science and Engineering C*, 2007, **27**, 262.
197. S. J. Liu, Y. C. Kau, C. Y. Chou, J. K. Chen, R. C. Wu, W. L. Yeh, *Journal of Membrane Science*, 2010, **355**, 53.
198. J. H. Song, H. E. Kim and H. W. Kim, *Journal of Materials Science: Materials in Medicine*, 2008, **19**, 2925.
199. J. Venugopal, S. Low, A. T. Choon, T. S. Sampath Kumar and S. Ramakrishna, *Journal of Materials Science: Materials in Medicine,* 2008, **19(5)**, 2039.
200. Z. G. Chen, P. W. Wang, B. Wei, X. M. Mo and F. Z. Cui, *Acta Biomaterialia*, 2010, **6**, 372.
201. H. M. Powell, D. M. Supp and S. T. Boyce, *Biomaterials,* 2008, **29**, 834.
202. C. P. Barnes, S. A. Sell, E. D. Boland, D. G. Simpson and G. L. Bowlin, *Advanced Drug Delivery Reviews*, 2007, **59**, 1413.
203. U. R. Rodgers, A. S. Weiss, *Pathologie Biologie,* 2005, **53**, 390.
204. L. Debelle, A. M. Tamburro, *International Journal of Biochemistry and Cell Biology,* 1999, **31**, 261.
205. E. N. Lamme, R. T. van Leeuwen, A. Jonker, J. van Marle and E. Middelkoop, *Journal of Investigative Dermatology,* 1998, **111**, 989.
206. S. Neuenschwander and S. P. Hoerstrup, *Transplant Immunology,* 2004, **12**, 359.
207. J. W. Xu, T. S. Johnson, P. M. Motarjem, G. M. Peretti, M. A. Randolph and M. J. Yaremchuk, *Plastic and Reconstructive Surgery,* 2005, **115**, 1633.
208. W. F. Daamen, J. H. Veerkamp, J. C. M. van Hest and T. H. van Kuppevelt, *Biomaterials,* 2007, **28**, 4378.
209. L. Nivison-Smith, J. Rnjak and A. S. Weiss, *Acta Biomaterialia,* 2010, **6**, 354.
210. S. G. Wise, M. J. Byrom, A. Waterhouse, P. G. Bannon, A. S. Weiss and M. K. Ng, *Acta Biomaterialia,* 2011, **7(1)**, 295.
211. K. A. McKenna, M. T. Hinds, R. C. Sarao, P. C. Wu, C. L. Maslen, R. W. Glanville, D. Babcock and K. W. Gregory, *Acta Biomaterialia,* 2012, **8(1)**, 225.
212. M. Li, M. J. Mondrinos, M. R. Gandhi, F. K. Ko, A. S. Weiss and P. I. Lelkes, *Biomaterials,* 2005, **26(30)**, 5999.
213. J. Rnjak, Z. Li, P. K. Maitz, S. G. Wise and A. S. Weiss, *Biomaterials*, 2009, **30(32)**, 6469.
214. J. Rnjak-Kovacina, S. G. Wise, Z. Li, P. K. Maitz, C. J. Young, Y. Wang and A. S. Weiss, *Biomaterials*, 2011, **32**, 6729.
215. J. Rnjak-Kovacina, S. G. Wise, Z. Li, P. K. Maitz, C. J. Young, Y. Wang and A., S. Weiss, *Acta Biomaterialia*, 2012, **8**, 3714.
216. S. G. Wise, M. J. Byrom, A. Waterhouse, P. G. Bannon, A. S. Weiss and M. K. Ng, *Acta Biomaterialia*, 2011, **7**, 295.

217. M. Li, M. J. Mondrinos, X. Chen M. R. Gandhi, F. K. Ko and P. I. Lelkes, *Journal of Biomedical Materials Research A.,* 2006, **79(4)**, 963.
218. L. A. Bosworth, *Conference Papers in Science*, 2014, Article ID:304974, http://dx.doi.org/10.1155/2014/304974.
219. ClinicalTrials Homepage: Available online at http://www.clinicaltrials.gov/ (accessed on 25 May 2014).
220. InVivo Therapeutics Homepage: Available online at http://www.invivotherapeutics.com/2013/04/invivo-therapeutics-receives-approval-from-fda-for-first-human-trial-using-biomaterials-for-traumatic-spinal-cord-injury/ (accessed on 22 May 2014).
221. Available online at http://www.nicast.com/index.aspx?id=2930 (accessed on 22 May 2014).
222. Nicast Homepage: Available online at http://www.nicast.com/index.aspx?id=2959 (accessed on 25 May 2014).
223. M. Stuart, *Start-up*, 2009, **14(8)**, 1. Available online at www.nuortho.com/assets/pdf/News_CartilageRepair0909su.pdf (accessed on 25 May 2014).
224. St Teresa Medical Inc. Homepage: Available online at http://www.stteresamedical.com/about_us.php (accessed on 25 May 2014).
225. Nanofiber Veterinary: Available online at http://nanofiberveterinary.com/nanocarev.html (accessed on 25 May 2014).
226. Nanofiber Veterinary: Available online at http://nanofiberveterinary.com/nanoligv.html (accessed on 25 May 2014).
227. Nanofiber Veterinary: Available online at http://nanofiberveterinary.com/nanovesselv.html (accessed on 25 May 2014).
228. Nanofiber Veterinary: Available online at http://nanofiberveterinary.com/nanobonev.html (accessed on 25 May 2014).

Table 1: Dependence of cellular response on cell type and nature of polymer.

Cell type (organ)	Polymer	Fiber diameter (FD) / pore size (PS)	Factor influencing cell growth	Cellular effect	References
Chondrocytes (cartilage)	PLA		• Fiber alignment • Crystallinity	• Cells exhibited a more elongated morphology in oriented PLLA scaffolds compared to non-oriented ones • Higher crystallinity suppresses cell proliferation and the cells produce higher amounts of ECM	Areis *et al.* [100]
	Chitosan	FD: 300, 500 and 1,030 nm	Fiber diameter	• Number of live chondrocytes on smaller diameter mat was higher compared to the larger diameter one	Noriega *et al.* [81]
Fibroblasts (skin)	PCL	PS: 6,8, 20 µm	Pore size	• Optimal pore size for proliferation of HDFs appears to be greater than 6 µm, but less than 20 µm.	Lowery *et al.* [82]
Keratinocytes (skin)	PVA	FD: 321.8 ± 89.3 nm PS: 2560 ± 1260 nm	• Contact angle • Thickness of scaffold • Pore size • Fiber orientation • 3D v/s 2D environment	• Poor cell adhesion on PVA film (CA = 63.1°) compared to electrospun fibers (CA = 54.2°) • Thicker scaffolds caused the cells to adopt a more rounded morphology • Cells grown on the electrospun scaffold were practically immobile in contrast to those on the glass cover slip • Cell growth directed by the orientation of nanofibers, and guide the cell migration and elongation • Higher metabolic activity on electrospun mat compared to glass slide	Pelipenko *et al.* [78]
Fibroblasts and keratinocytes (skin)	PHB PVA/PHB	FD pure PHB: 680 nm FD 50/50 PVA/PHB: 615 nm	Contact angle Pure PHB: 70° 50/50 PVA/PHB: 41°	Decreased number of viable fibroblasts and enhanced adhesion and proliferation of keratinocytes with increasing PVA content	Asran *et al.* [101]
	Chitin	FD nanofibers: 163 nm FD microfibers: 8.77 µm	Fiber diameter	Higher cell attachment and spreading of cells on nanofibers compared to microfibers	Noh *et al.* [102]
Osteoblasts (bone)	Gelatin	FD: 110 ± 40 nm and 600 ± 110 nm	Fiber diameter	• Poor migration of MG63 cells in small diameter scaffold (maximum depth of 18 µm) compared to larger diameter scaffold (maximum depth of 50 µm). • MG63 cell differentiation favored on small diameter scaffolds compared to large diameter ones at days 3 and 7, but the ALP levels were the same for both scaffold types by day 14.	Sisson *et al.* [85]
	PLLA	FD random fibers: 450 nm FD aligned fibers: 275 nm PS random fibers: 2.2 µm PS aligned fibers: 1.0 µm	Fiber alignment	• Cells had irregular polygonal forms on random mats while those on aligned nanofibers exhibited shuttle-like shapes • Lowest and highest ALP activity observed random and aligned mats respectively • Higher cell infiltration in random mats	Wang *et al.* [79]
	PDLA	FD: 0.14, 2.1 µm	Fiber diameter	Cells on 2.1µm diameter fibers exhibited a higher aspect ratio (contact guidance) compared to the 0.14 µm fibers	Badami *et al.* [83]
	PCL	FD: 930 nm and 5.0 µm	Fiber diameter	Higher ALP activity observed on microfiber compared to nanofibers	Li *et al.* [84]

Table 2: *In vitro* cell culture studies on electrospun PCL and PCL-blend nanofibers.

Cell type	Seeding density/cells per cm^2	Sterilization method	Results	Time (cell viability)	Average fiber diameter/nm	References
PCL						
Fetal bovine chondrocytes (FBCs)	1×10^4 4×10^5	UV radiation	MTS assay revealed a 21-fold increase in cell growth over 21 days when the cultures were maintained in serum-containing medium compared to TCPS.	21 days	700	Li *et al.* [117]
Neonatal Lewis rat cardiomyocytes	2.5×10^6	70% ethanol	Started beating after 3 days; good attachment of cardiomyocytes; Expressed cardiac-specific proteins such as α-myosin heavy chain, connexin43 and cardiac troponin I.	14 days	-	Shin *et al.* [118]
Neonatal Lewis rat cardiomyocytes	2.5×10^6	-	Good attachment of cultured cardiomyocytes, and strong beating was observed.	14 days	100-5000	Ishii *et al.* [119]
Human bone marrow MSCs	4×10^5	UV radiation	MSCs cultured in NFSs in the presence of TGF-β1 differentiated to a chondrocytic phenotype, as evidenced by chondrocyte-specific gene expression and synthesis of cartilage-associated extracellular matrix (ECM) proteins. The level of chondrogenesis observed in MSCs seeded within scaffolds was comparable to that observed for MSCs maintained as cell aggregates or pellets.	21 days	500-900	Li *et al.* [120]
Human MSCs	2.5×10^5	UV radiation	With increasing, rotating speed, cell morphology changed from pyramidal to more elongated cells, with actin aligned in the direction of the fibers.	28 days	700	Li *et al.* [121]
Rat brain derived neural stem cells	5×10^5 cells/ mL	70% ethanol	Stem cells primarily differentiated into oligodendrocytes, showing the ability of PCL to direct differentiation of cells into a specific lineage.	7 days	750	Nisbet *et al.* [122]
Human dermal fibroblasts	5×10^5 cells/ mL	-	LIVE–DEAD staining of scaffolds at 14 days revealed primarily live cells, with little evidence of dead cells. Cell counts close to 6×10^6 cells/scaffold after 21 days.	21 days	730-10530	Lowery *et al.* [82]
PCL/collagen						
Human coronary smooth muscle cells	4×10^4	Ethanol	SMCs migrated towards inside the nanofibrous matrices and formed smooth muscle tissue	3 days	300-600	Venugopal *et al.* [123]
Human dermal	1×10^4	Ethanol	Cell proliferation was lower on PCL nanofibrous	6 days	250-275	Venugopal *et al.*

fibroblasts			membrane compared to PCL/collagen membrane.			[124]
Human bone marrow derived MSCs	3×10^4	Oxygen plasma	Supported cell attachment in a way similar to traditionally used TCPS.	6 weeks	-	Srouji *et al.* [125]
Human skeletal muscle cells (hSkMCs)	4×10^4	Ethylene oxide	Electrospun PCL/collagen nanofibers guided and oriented skeletal muscle cells into organized structures. Unidirectional oriented nanofibers significantly induced muscle cell alignment and myotube formation as compared to randomly oriented nanofibers.	7 days	Random: 334 Aligned: 296	Choi *et al.* [126]
Human dermal fibroblasts	1×10^5 cells/ mL	-	High cell adhesion (88.2%) and rapid cell spreading with spindle-like morphology was observed on the nanofiber surface.	1 day	455	Yang *et al.* [127]
(1) Human aortic smooth muscle cells (external surface) (2) Human aortic endothelial cells (onto lumen)	(1) 5×10^4 cells/ mL (2) 4×10^4 cells/ mL	Ethylene oxide	(1) Cells infiltrated the scaffold (2) Cells adhered and spread over multiple fibers	4 weeks	270-4450	Ju *et al.* [128]
PCL/gelatin						
Rat bone marrow stromal cells (BMSCs)	2×10^4	UV radiation	Cells could not only favorably attach and grow well on the surface of these scaffolds, but were also able to migrate inside the scaffold up to 114 μm within 1 week of culture.	1 week	10-1000	Zhang *et al*. [129]
Human coronary artery endothelial cells	2.5μM/mL, 200μL/ well	75% ethanol	Immunostaining micrographs showed that the cells were able to maintain the expression of three characteristic markers: platelet-endothelial cell adhesion molecule 1 (PECAM-1), intercellular adhesion molecule 1 (ICAM-1), and vascular cell adhesion molecule 1 (VCAM-1).	4 days	200-1000	Ma *et al*. [130]
Human dermal fibroblasts	1×10^4 cells/ well	UV radiation and 70% ethanol	Successful HDF proliferation and adherence on scaffold; however, not much significant fibroblast infiltration within the scaffold structure.	7 days	470	Chong *et al.* [131]
L 929 mouse fibroblasts	1×10^5 cells/ well	70% ethanol	Proliferation of L929 cells was as good as on TCPS. Morphology of cells was fibroblastic.	7 days	488-663	Tigli *et al.* [132]

L 929 mouse fibroblasts	2×10^5 cells/ mL	UV radiation	PCL/gelatin composite nanofibrous scaffold showed the percentage cell viability of 96.8%, 97.1% and 98.4% at 24, 48 and 72 h, respectively, whereas the PCL nanofibrous scaffold showed reduced cell viability of 93.5%, 93.8% and 94.5% at 24, 48 and 72 h respectively, under similar experimental conditions.	3 days	291-1173	Gautam *et al.* [133]
Mouse embryonic stem cells	5×10^3 cells/ mm^2	-	Cell growth and attachment were supported.	3 days	570	Lim *et al.* [134]
PCL/HA						
Murine embryonic stem cells	8×10^4	70% ethanol	Cells proliferated and maintained pluripotency markers at essentially the same rate as cells growing on standard tissue culture plates with no detectable signs of cytotoxicity, despite a lower cell adhesion at the beginning of culture.	3 days	1500	Bianco *et al.* [135]
Bone marrow mesenchymal stem cells	1×10^5 cells/ well	-	Supported the growth of mesenchymal stem cells without compromising their osteogenic differentiation capability for up to 21 days. The ALP activity of cells in PCL/50% HA scaffold was 2.7 and 1.8 times higher than in PCL and in PCL/25% HA scaffolds at day 21 respectively.	21 days	340	Chen *et al.* [136]
PCL/chitin						
Human dermal fibroblasts	1×10^5 cells/ well	Ethanol	Cells not only spread on the surface of scaffold, but also penetrated and migrated inside the scaffold.	14 days	200-400	Ji *et al.* [137]
PCL/fucoidan						
Osteoblast-like cells (MG63)	1×10^5	-	Cells were distributed more widely and were agglomerated on PCL/fucoidan mats compared to pure PCL mats. Total protein content, ALP activity and calcium mineralization were higher with PCL/fucoidan mats than with pure PCL mats.	10 days	500	Lee *et al.* [138]

Table 3: *In vivo* studies on electrospun PCL or PCL based nanofibers.

Animal Model	Organ/ Tissue	Results	References
PCL			
Rat	Omenta	After 4 weeks of *in vitro* culture, the scaffolds were implanted. Cells and ECM formation were observed throughout the constructs. In addition, mineralization and type I collagen were also detected after 4 weeks.	Shin *et al.* [139]
	Abdominal aorta	Good patency, endothelization, and cell ingrowth were observed following the 12-week implantation period.	Nottelet *et al.* [140]
	Abdominal aorta	Digital subtraction angiography revealed no stenosis in the PCL group but stenotic lesions in 1 graft at 18 weeks (40%). Macrophage and fibroblast ingrowth with ECM formation and neoangiogenesis were better in the PCL group compared to ePTFE. After 12 weeks, foci of chondroid metaplasia located in the neointima of PCL grafts were observed in all samples.	Pektok *et al.* [141]
	Cranial bone	*In vivo* results after 6 months exhibited osseous tissue integration within the implant and mineralized bone restoration of the calvarium.	Piskin *et al.* [142]
	Caudate putamen of brain	Neurites infiltrated the implants, providing evidence of scaffold-neural integration.	Nisbet *et al.* [143]
	Skin	Thicknesses of fibrous capsule on fibrous scaffolds were 7.55±0.54 micron for aligned fibers and 4.13±0.31 micron for random fibers, which were significantly thinner than that of film implants 37.7±0.25 micron ($p < 0.001$).	Cao *et al.* [144]
	Sciatic nerve	Microscopic examination of the regenerating tissue revealed dense, parallel arrays of myelinated and non-myelinated axons, 7 weeks post-implantation	Jha *et al.* [145]
Swine	Cartilage	After 6 months, the MSC-seeded PCL constructs regenerated hyaline cartilage-like tissue and restored a smooth cartilage surface. No evidence of immune reaction to the regenerated cartilage was observed, possibly related to the immunosuppressive activities of MSCs.	Li *et al.* [146]
PCL-collagen			
Rabbit	Corpus cavernosa	After 3 months, PCL/collagen scaffolds used in conjunction with autologous smooth muscle cells resulted in better integration with host tissue when compared to cell free scaffolds. On a cellular level pre-seeded scaffolds showed a minimized foreign body reaction.	Chen *et al.* [147]
	Aortoiliac artery	Scaffolds were able to retain their structural integrity over 1 month of implantation as demonstrated by serial ultrasonography. At retrieval, scaffolds continued to maintain biomechanical strength that was	Tillman *et al.* [148]

		comparable to native artery.	
Mice	Skin	Good integration with the surrounding tissues and neovascularization.	Srouji *et al.* [125]
PCL-*b*-PEG-*b*-PCL			
Rabbit	Calvarial bone	New bone formed originally from the margin of host bone and then grew towards the center of defects. At 20th week, the defects of treatment group were covered with the new solid cortical bone.	Fu *et al.* [149]

Table 4: *In vitro* cell culture studies on electrospun PLA and PLA-blend nanofibers.

Cell type	Seeding density/cells per cm^2	Sterilization method	Results	Time (cell viability)	Average fiber diameter/nm	References
PLA						
Pre-osteoblast cells (MC3T3-E1)	-	Ethanol	The bone mineralized protein-2 (BMP-2) and osteocalcin (OCN) expressions from cells on the melt electrospun PLA fibers were 6-fold and 1.8-fold greater than those on the solution electrospun fibers respectively, due to the solvent-free condition. In addition, melt electrospun fibers provide a significantly higher cell-viability, approximately 2-fold greater than solution electrospun fibers.	7 days	1500	Lee *et al.* [159]
PDLA						
Human embryonic stem cells (hESC)	1×10^5	-	Attached cells started to migrate and maturate within 3 days in culture. hESC derived neurons grow and mature well on 3D PDLA scaffolds.	7 days	800-5000	Ylä-Outinen *et al.* [160]
PLGA						
Human mesenchymal stem cells (hMSCs)	2×10^6 cells/ mL	-	The majority of hMSCs was viable and proliferating in PLGA nanofiber scaffolds up to the tested 14 days.	14 days	760	Xin *et al.* [161]

PLA-HA						
Rat osteosarcoma ROS17/2.8 cells	2×10^4	-	All the HA/PLLA nanofibrous scaffolds studied exhibited good biocompatibility and cell signaling properties. Compared with a PLLA scaffold, the HA/PLLA scaffolds demonstrated better support for cell attachment, proliferation and differentiation.	10 days	300	Peng *et al*. [162]
Human fetal osteoblasts (hFOB)	10×10^3	-	hFob cells were found to proliferate better on PLLA/HA scaffolds than on PLLA scaffolds. Mineralization increased from day 10 to day 20 and was found to be higher on PLLA/HA scaffolds than on PLLA scaffolds.	20 days	845	Prabhakaran *et al.* [163]
Osteoblast cell (MG-63)	-	-	Cell adhesion and growth on the PLLA/HA hybrid mats were far better than those on the pure PLLA mats.	5 days	313	Sui *et al.* [164]
PLA-Tricalcium phosphate						
Human adipose-derived stem cells (hASCs)	2×10^4	-	Human ASCs were able to adhere, proliferate and osteogenically differentiate on all scaffold combinations.	18 days	503-1267	McCullen *et al.* [165]
PLA-gelatin						
Dermal fibroblast cell lines	10,000	UV radiation	Gelatin/PLLA nanofibrous mat showed excellent *in vitro* biocompatibility.	4 days	77.3-147.7	Gu *et al.* [166]
Primary human chondrocytes	2.5×10^5 cells/ mL	-	Cells grown on the scaffolds exhibit good proliferation and increased values of the differentiation parameters, especially for intermediate PLLA/GEL compositions.	14 days	PLLA fiber diameter = 560 nm; gelatin fiber diameter =500 nm.	Torricelli *et al.* [167]
PLA-PCL						
Human adipose-derived stem cells (hASCs)	5×10^5 cells/ mL	-	Scaffolds supported hASCs well. However, the 1/1 wt ratio PLA/PCL showed better properties and cellular responses in all assessments.	7 days	682-1250	Chen *et al.* [168]

P(LA-CL)						
Smooth muscle cells and endothelial cells	1–5×10^5	Ethanol	Both SMC and EC adhered and spread on the nanofiber surface, they interacted and integrated well with the surrounding fibers.	7 days	450-600	Mo *et al.* [169]
PLGA-HA						
Neonatal mouse calvaria-derived MC3T3-E1 osteoblasts	4×10^4 cells/ well	-	Cells cultured on the PLGA/5HAp scaffolds showed significantly higher ALP activity than that on the control PLGA scaffolds by a factor of 60% at 7 days.	14 days	267	Lao *et al.* [170]

Table 5: *In vivo* studies on electrospun PLA or PLA based nanofibers.

Animal Model	Organ/ Tissue	Results	References
PLA			
Rat	Calvarial bone	Bone regeneration was significantly increased *in vivo* and after 12 weeks osteocalcin, BMP-2 and Smad5 were all significantly higher in the PLLA/BMP-2 group than in all other groups. No histological foreign body reaction was noted with either PLLA or PLLA/BMP-2 implants.	Schofer *et al.* [171]
PLA-PCL			
Rat	Dorsal pocket	At 1 week after implantation, the scaffolds were surrounded by a large number of CD68+ macrophagocytes. The number of macrophagocytes decreased with time, and then vanished at 4 weeks, which meant the inflammation reaction ended.	Chen *et al.* [168]

Table 7: *In vitro* cell culture studies on electrospun collagen-blend nanofibers.

Cell type	Seeding density/cells per cm^2	Sterilization method	Results	Time (cell viability)	Average fiber diameter/nm	References
Collagen						
Aortic smooth muscle cells	5×10^5 cells/ mL	-	The scaffolds were densely populated with the smooth muscle cells within 7 days.	7 days	390	Matthews *et al.* [191]

Chondrocytes	5–10×10^6	-	Cells were able to infiltrate the scaffold surface and interior.	7 days	Uncrosslinked fibers: 496 Crosslinked fibers: 1460	Shields *et al.* [192]
Human keratinocytes	1×10^5	-	Relatively low cell adhesion was observed on uncoated collagen nanofibers, whereas collagen nanofibrous matrices treated with type I collagen or laminin were functionally active in responses in normal human keratinocytes.	7 days	460	Rho *et al.* [193]
Rabbit conjunctiva fibroblast	5×10^4 cells/ well	Ethanol	Aligned collagen scaffold exhibited lower cell adhesion but higher cell proliferation compared to the random one.	7 days	180, 250	Zhong *et al.* [194]
Human bone marrow-derived mesenchymal stem cells (BMSCs)	3,000	UV radiation	Cells grown on larger diameter nanofibers (500-1000 nm) had significantly higher cell viability than the TCPS control. Type I collagen nanofibers supported the growth of BMSCs without compromising their osteogenic differentiation capability.	12 days	50-1000	Shih *et al.* [195]
Collagen-glycosaminoglycan						
Rabbit conjunctiva fibroblasts	1×10^4 cells/ well	UV radiation	Cell density on collagen/glycosaminoglycan scaffold was significantly greater than on collagen scaffold.	7 days	260	Zhong *et al.* [196]
Collagen-PLGA						
Human fibroblasts	5×10^3 cells/ well	-	A high level of cell adhesion was observed on the surface of the matrix at 1 week and in-depth cell growth was noted at 2 weeks.	2 weeks	170-650	Liu *et al.* [197]
Collagen-HA						
Pre-osteoblast cell line MC3T3-E1	1.5×10^4	-	The MC3T3-E1 osteoblastic cells were shown to adhere and grow actively on the collagen–HA nanofibrous web. The alkaline phosphatase (ALP) activity expressed by the cells on the collagen–20 wt%HA nanofiber was lower at day 7, but was higher at day 14 than that on the pure collagen	14 days	70-170	Song *et al.* [198]

			nanofiber.			
Osteoblasts	2×10^4	-	Osteoblasts cultured on both scaffolds and show insignificant level of proliferation but mineralization was significantly ($p < 0.001$) increased to 56% in Col/HA nanofibrous scaffolds compared to collagen	6 days	293	Venugopal *et al.* [199]
Collagen-chitosan						
(1) Endothelial cells (EC) (2) Smooth muscle cells (SMC)	(1) 4×10^3 (2) 3×10^4	75% radiation	Both EC and SMC spread well on the surface of the nanofiber and cells interacted and integrated well with the surrounding fibers. Cells also migrated and proliferated in certain patterns and formed a continuous monolayer.	14 days	434-691	Chen *et al.* [200]

Table 8: *In vivo* studies on electrospun collagen or collagen based nanofibers.

Animal Model	Organ/ Tissue	Results	References
Collagen			
Mice	Skin	At 2 weeks after surgery, scaffolds were well-integrated into surrounding murine skin and possessed a uniformly dry epidermis. Fibroblasts and keratinocytes were well stratified on scaffolds with a continuous basal layer of keratinocytes. A layer of cornified keratinocytes was also forming.	Powell *et al.* [201]

Table 9: *In vitro* cell culture studies on electrospun elastin-blend nanofibers.

Cell type	Seeding density/cells per cm^2	Sterilization method	Results	Time (cell viability)	Average fiber diameter/nm	References
Elastin						
(1) Human fibroblasts (2) Primary human	(1) 2.5×10^4 (2) 5×10^4	-	Good cell attachment and proliferation	24 hours	1800	Nivison-Smith *et al.* [209]

umbilical vein endothelial cells (HUVECs) (3) human coronary artery smooth muscle cells (HCASMCs)	(3) 5×10^4					
Human umbilical vein endothelial cells	300 cells/ mm^2	-	Tropoelastin enhanced endothelial cell attachment (threefold vs. control) and proliferation by 54.7 ± 1.1% (3 days vs. control).	3 days	-	Wise *et al.* [210]
Bone marrow derived endothelial outgrowth cells (BMEOCs)	5×10^3	-	Endothelial cell growth with typical endothelial cell cobblestone morphology was observed after 48 h in culture. Confocal images showed that cells attached well and spread on the electrospun fiber matrix.	2 days	580	McKenna *et al.* [211]
Human embryonic palatal mesenchymal cells (HEPM)	20,000 cells/ sample	Ethanol	HE PM cells attached, spread, migrated, and proliferated to confluence equally well on collagenous scaffolds as on the scaffolds made of elastin.	6 days	200-500	Li *et al.* [212]
Primary human dermal fibroblasts	5×10^4	-	Cells attached and proliferated to form monolayers spanning the entire scaffold surface.	14 days	2.3 ±0.5 µm prior to cross-linking and 3.4 ±0.8 µm following GA cross-linking	Rnjak *et al.* [213]
Primary human dermal fibroblasts	5×10^4/ cm^2	-	Low and high porosity scaffolds supported early attachment, spreading and proliferation of primary dermal fibroblasts, but only high porosity scaffolds supported active cell migration and infiltration into the scaffold.	35 days	2.3±0.5 µm when electrospun at 1 mL/h compared to 3.2 ± 1.0 µm at 3 mL/h.	Rnjak-Kovacina *et al.* [214]
Elastin-collagen						
Dermal fibroblasts	2×10^5/ scaffold	-	Enhanced proliferation and migration rates of dermal fibroblasts were observed.	8 days	1100-6500	Rnjak-Kovacina *et al.* [215]

Elastin-PCL						
Human umbilical vein endothelial cells (HUVECs)	300 cells/ mm^2	-	HUVECs attached to and spread on all of the scaffold surfaces by day 3.	5 days	-	Wise *et al.* [216]
PLGA-gelatin-elastin						
H9c2 rat cardiac myoblasts and rat bone marrow stromal cells (BMSCs)	500,000/ mL	-	Myoblasts grew slightly better on the scaffolds than on TCPS, reaching confluence on the scaffold surfaces while simultaneously growing into the scaffolds. BMSCs penetrated into the center of scaffolds and began proliferating shortly after seeding.	8 days	380	Li *et al.* [217]

Table 10: *In vivo* studies on electrospun elastin or elastin based nanofibers.

Animal Model	Organ/Tissue	Results	References
Elastin			
Mouse	Skin	The scaffolds persisted for at least 6 weeks, with fibroblasts on the exterior and infiltrating, evidence of scaffold remodeling including de novo collagen synthesis and early stage angiogenesis.	Rnjak-Kovacina *et al.* [214]
Elastin-collagen			
Mouse	Skin	The scaffolds generated a mild inflammatory response. However, this did not prevent dermal fibroblast infiltration, and de novo collagen deposition which was observed throughout the scaffolds over the 6 weeks study.	Rnjak-Kovacina *et al.* [215]
Elastin-PCL			
Rabbit	Carotid artery	Animals recovered well from surgery and displayed normal characteristic behavior including mobility and feeding until the study end-point. After explantation at 1 month, the grafts showed no evidence of dilatation, anastomotic dehiscence or seroma.	Wise *et al.* [216]

Table 11: Clinical trials on the use of electrospun nanofibers for tissue engineering.

ClinicalTrials.gov Identifier	Clinical trial name	Details	Tissue	Status/Phase
NCT02138110	Pilot Study of Clinical Safety of the PLGA Poly-L-Lysine Scaffold for the Treatment of Complete (ASIA A) Traumatic Acute Spinal Cord Injury	Poly(lactide-*co*-glycolide) biodegradable scaffolds seeded with neural stem cells	Spinal cord	Currently recruiting participants
NCT01849458	BioFiber and BioFiber-CM Absorbable Biologic Scaffold for Soft Tissue Repair and Reinforcement Post-Market Surveillance Clinical Study	Matrix consisting of collagen and P4HB	Soft tissue repair	Ongoing
NCT01041885	Prospective Feasibility, Non-randomized, Single Arm Multicentre, Multinational Interventional Clinical Investigation Using INSTRUCT Therapy for the Repair of Knee Cartilage Defects	Isolated primary chondrocytes with autologous bone marrow cells seeded onto a polymeric scaffold	Cartilage repair	Ongoing

Journal Name RSCPublishing